



**HAL**  
open science

## A review of recent progress on electrocatalysts toward efficient glycerol electrooxidation

Peter Adeniyi Alaba, Ching Shya Lee, Faisal Abnisa, Mohamed Kheireddine Aroua, Patrick Cognet, Yolande Peres-Lucchese, Wan Mohd Ashri Wan Daud

### ► To cite this version:

Peter Adeniyi Alaba, Ching Shya Lee, Faisal Abnisa, Mohamed Kheireddine Aroua, Patrick Cognet, et al.. A review of recent progress on electrocatalysts toward efficient glycerol electrooxidation. *Reviews in Chemical Engineering*, 2020, 36, pp.1-34. 10.1515/revce-2019-0013 . hal-02540005

**HAL Id: hal-02540005**

**<https://hal.science/hal-02540005v1>**

Submitted on 10 Apr 2020

**HAL** is a multi-disciplinary open access archive for the deposit and dissemination of scientific research documents, whether they are published or not. The documents may come from teaching and research institutions in France or abroad, or from public or private research centers.

L'archive ouverte pluridisciplinaire **HAL**, est destinée au dépôt et à la diffusion de documents scientifiques de niveau recherche, publiés ou non, émanant des établissements d'enseignement et de recherche français ou étrangers, des laboratoires publics ou privés.






## Open Archive Toulouse Archive Ouverte (OATAO)

OATAO is an open access repository that collects the work of Toulouse researchers and makes it freely available over the web where possible

This is an author's version published in: <http://oatao.univ-toulouse.fr/25853>

**Official URL:** <https://doi.org/10.1515/revce-2019-0013>

**To cite this version:**

Alaba, Peter Adeniyi and Lee, Ching Shya  and Abnisa, Faisal and Aroua, Mohamed Kheireddine and Cognet, Patrick  and Peres-Lucchese, Yolande  and Wan Daud, Wan Mohd Ashri *A review of recent progress on electrocatalysts toward efficient glycerol electrooxidation.* (2020) *Reviews in Chemical Engineering*, 36. 1-34. ISSN 0167-8299

Any correspondence concerning this service should be sent to the repository administrator: [tech-oatao@listes-diff.inp-toulouse.fr](mailto:tech-oatao@listes-diff.inp-toulouse.fr)

Peter Adeniyi Alaba\*, Ching Shya Lee\*, Faisal Abnisa, Mohamed Kheireddine Aroua, Patrick Cagnet, Yolande Pérès and Wan Mohd Ashri Wan Daud\*

# A review of recent progress on electrocatalysts toward efficient glycerol electrooxidation

**Abstract:** Glycerol electrooxidation has attracted immense attention due to the economic advantage it could add to biodiesel production. One of the significant challenges for the industrial development of glycerol electrooxidation process is the search for a suitable electrocatalyst that is sustainable, cost effective, and tolerant to carbonaceous species, results in high performance, and is capable of replacing the conventional Pt/C catalyst. We review suitable, sustainable, and inexpensive alternative electrocatalysts with enhanced activity, selectivity, and durability, ensuring the economic viability of the glycerol electrooxidation process. The alternatives discussed here include Pd-based, Au-based, Ni-based, and Ag-based catalysts, as well as the combination of two or three of these metals. Also discussed here are the prospective materials that are yet to be explored for glycerol oxidation but are reported to be bifunctional (being capable of both anodic and cathodic reaction). These include heteroatom-doped metal-free electrocatalysts, which are carbon materials doped with one or two heteroatoms (N, B, S, P, F, I, Br, Cl), and heteroatom-doped nonprecious transition metals. Rational design of these materials can produce electrocatalysts with activity comparable to that of Pt/C

catalysts. The takeaway from this review is that it provides an insight into further study and engineering applications on the efficient and cost-effective conversion of glycerol to value-added chemicals.

**Keywords:** acidic media; alkaline media; electrocatalyst; glycerol electrooxidation; platinum.

## 1 Introduction

Fossil fuel consumption and depletion are increasing progressively because of the ever-increasing global energy demand as well as the need to alleviate emission of greenhouse gases (Silva et al. 2017). In this regard, it is essential to develop more sustainable and renewable alternatives to fossil fuel resources for satisfying global energy needs (Houache et al. 2018). One of the considered alternatives is biodiesel, which is technically, economically, and environmentally viable. Biodiesel is a product of transesterification of animal fats or vegetable oils, which produces glycerol (about 10 wt%) as a byproduct (Suzuki et al. 2016). Though glycerol is exploited as a raw material in the tobacco, cosmetics, food, and pharmaceutical industries, the supply of glycerol is much higher than the demand because of the growth of the biodiesel industry. The abundance of glycerol has propelled the search for more routes for glycerol transformation into specialty chemicals to make biodiesel production cheaper and more environmentally benign (Oliveira et al. 2015).

Electrooxidation of glycerol is a promising route for the transformation of glycerol into specialty chemicals. The reaction pathway for the electrooxidation of glycerol in alkaline electrolytes is complex (Katryniok et al. 2011). This process uses the produced electrons and holes to perform the reaction by combining the hydrogen generated at the cathode and the specialty chemicals formed at the anode using an appropriate potential (Dodekatos et al. 2018). Several useful intermediates/oxygenated species such as glycolate, glycerate, tartronate, hydroxypyruvate, glycolic acid, mesoxalic acid oxalate, mesoxalate, dihydroxyacetone, and formate ions are formed. Some authors have reported a mixture of these intermediates in the glycerol

---

\*Corresponding authors: Peter Adeniyi Alaba and Wan Mohd Ashri

Wan Daud, Department of Chemical Engineering, University of Malaya, 50603 Kuala Lumpur, Malaysia,

e-mail: adeniyipee@live.com (P.A. Alaba); ashri@um.edu.my

(W.M.A.W. Daud). <https://orcid.org/0000-0003-3552-6718>

(P.A. Alaba); and Ching Shya Lee, Department of Chemical Engineering, University of Malaya, 50603 Kuala Lumpur, Malaysia; and UMR5503 Laboratoire de Génie Chimique (LGC), Toulouse, France, e-mail: leecs@um.edu.my

Faisal Abnisa: Department of Chemical Engineering, King Abdulaziz University, Rabigh 21911, Saudi Arabia

Mohamed Kheireddine Aroua: Research Centre for Nanomaterials and Energy Technology (RCNMET), School of Science and Technology, Sunway University, Bandar Sunway 47500, Malaysia; and Department of Engineering, Lancaster University, Lancaster, LA1 4YW, UK

Patrick Cagnet and Yolande Pérès: UMR5503 Laboratoire de Génie Chimique (LGC), Toulouse, France

electrooxidation reaction (GEOR) (Zhang et al. 2012b). Some of these products could be utilized as drug delivery agents, heavy-metal complexing agents, or polymer raw materials. Presently, these specialty chemicals are mostly synthesized either via slow fermentation processes resulting in low product yields (Bauer and Hekmat 2006) or environmentally unfriendly and costly stoichiometric oxidation processes (Carrettin et al. 2003). The transformation of glycerol occurs in the presence of oxygen, which plays a significant role in the heterogeneous catalytic oxidation of glycerol, just like in the  $O_2$  reduction reaction (ORR) at the cathode region of the fuel cell. Nevertheless, because of the restrictions in the nature and design of traditional batch reactors, the catalytic oxidation process involves the wastage of glycerol's chemical energy ( $6.3 \text{ kWh l}^{-1}$ ), which could be converted to heat during oxidation. Transformation of glycerol in a direct alcohol fuel cell (DAFC) has the potential to produce several specialty chemicals and generate electrical energy simultaneously at a lower theoretical energy density ( $5.0 \text{ kWh kg}^{-1}$ ) when compared with methanol and ethanol ( $6.1$  and  $8.1 \text{ kWh kg}^{-1}$ , respectively) (Holade et al. 2013a,b, Gomes et al. 2014a).

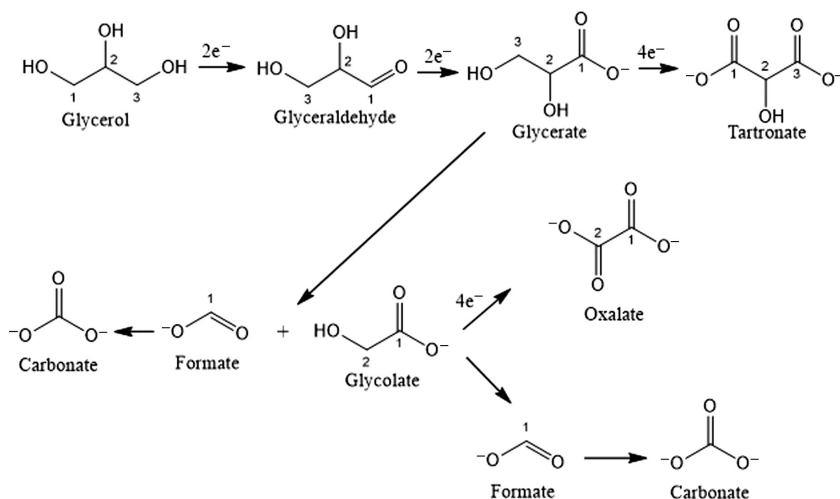
Several researchers have studied GEOR using noble metals such as Au, Pt, and Pd (Zalineeva et al. 2014, Garcia et al. 2015, 2017). They have been found to show satisfactory activity, but the selectivity of the desired products needs to be improved. For instance, the formation of C3 products such as mesoxalic and tartronic acid is difficult by further oxidation (Zhang et al. 2012b). Several reviews have been written on glycerol oxidation. Simões et al. (2012) gave an overview of the principle of glycerol electrooxidation, highlighting the advantages and drawbacks, relevant research, and remarkable results. Recently,

Dodekatos et al. (2018) reviewed the newly developed supported noble-metal NP catalysts as well as nonprecious catalysts. This review reveals the state of the art toward improving the selectivity of value-added chemicals. Several modifications on the above-mentioned noble metals are critiqued, as well as the synergistic combination of two or more metals (multimetallic catalysts).

## 2 Electrooxidation of glycerol and products

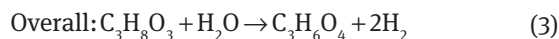
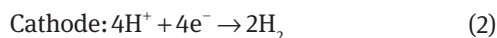
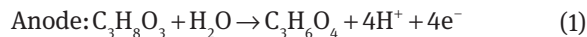
Electrooxidation of glycerol can be used to produce electrical energy (Kim et al. 2011b, Zhang et al. 2012b) and oxidized compounds (Lee et al. 2016). Selective electrooxidation technology employs an ion exchange membrane and oxidation chemistry for the electrocatalytic transformation of glycerol to specialty chemicals (Kwon et al. 2011b, Simões et al. 2012). This process has been successfully used to convert glycerol to glyceric acid (GLA) and glyceraldehyde (GLAD) even without the use of a stoichiometric chemical oxidant such as  $H_2O_2$  or  $O_2$  in GEOR (Kim et al. 2017). When compared to the operating cost of the conventional heterogeneous catalytic reactor, that of a GEOR reactor is less because of the simplicity of the reaction process and the reactor design.

The rate of reaction and selectivity toward the desired products can be enhanced by varying the glycerol-to-catalyst ratio and tuning the electrode potential. Unlike in the conventional catalytic process, hydrogen gas is formed as a byproduct at the cathode side in GEOR (Frota et al. 2017, Kim et al. 2017). This hydrogen can be converted into heat



**Scheme 1:** Reaction pathway for glycerol electrooxidation in alkaline electrolytes (Kang et al. 2017). Reproduced with kind permission from Elsevier (copyright license no. 4663440703527).

and electricity or used in a reduction reaction. Typically, the following reactions occur during GEOR (Scheme 1):



At the anode, GLA, electrons, and protons are produced. Meanwhile, the electrons produced by water serve as the stoichiometric oxidant to produce the acid. The protons migrate to the cathode through the electrolyte in the reactor where they are transformed to  $\text{H}_2$  by combining with the electrons (Kim et al. 2017). Table 1 presents the typical oxidation products and their applications.

## 3 Types of electrocatalysts

### 3.1 Platinum-based electrocatalysts

Electrooxidation of glycerol on a Pt surface has been studied extensively both at a fundamental level and in applied research (Gomes et al. 2013). Pt is the first noble metal that was studied by Kimura and coworkers in 1993 as a catalyst in GEOR (Kimura 1993). GEOR proceeds by the interaction of  $\text{OH}^-$  in alkaline solutions, and the regeneration of the  $\text{OH}^-$  loop occurs through a four-electron transfer process in an oxygen atmosphere. Several authors have studied the GEOR mechanism. Falase et al. (2012) and Fernández et al. (2012b) studied glycerol oxidation on Pt electrodes in acid and alkaline solutions using cyclic voltammetry, online electrochemical mass spectrometry, and high-performance liquid chromatography. The main product observed was glyceric acid, while glyceraldehyde was the reactive intermediate (Fernández et al. 2013). The Pt surface is suitable for GEOR and can break the carbon chain to form formic acid and glycolic acid, leading to  $\text{CO}_2$  generation. The selectivity and activity of the Pt-based catalyst mainly depend on the surface structure, which further depends on the preparation method. Pt-based catalysts with larger NPs are known for their remarkable reaction rates and promote oxidation at the glycerol terminal carbons; cuboctahedral Pt-based NPs are more active than tetrahedral Pt-based NPs, but there is no significant difference in the selectivity (Li and Zaera 2015). Pt-based colloidal NPs are more selective toward glyceraldehyde. However, the activity of colloid-based catalysts declines

fast after short reaction times; therefore, colloid-based Pt catalysts must be modified or functionalized for better performance (Aliaga et al. 2009, Niu and Li 2013). To show the effect of the preparation method, Li and Zaera (2015) prepared three series of Pt/ $\text{SiO}_2$  catalysts by varying the metal loading and using different solvents and shapes of the premade metal NPs. The microstructural image is presented in Figure 1. They reported that metal loading influences the average size of the metal NPs, which affects both selectivity and activity. The intrinsic activity improves with increase in the size of the NPs, thereby favoring oxidation at the terminal alcohol groups of the glycerol to produce glyceraldehyde as an intermediate. In the study of Kwon et al. (2012), glycolic acid (two carbons) and formic acid (one carbon) were observed on the Pt surface. Upon modifying the surface of Pt with bismuth, glyceric acid, glyceraldehyde, and dihydroxyacetone (DHA) were mainly observed.

Schnaidt et al. (2011) reported that glycerol adsorption on the Pt surface cannot occur at potentials  $\leq 0.1$  V since  $\text{H}_{\text{upd}}$  inhibits GEOR. At potentials above 0.2 V, dissociation of glycerol occurs in adsorbed CO and other species, blocking the surface to prevent Pt-OH formation. They also reported the formation of glyceric acid at potentials between 0.6 and 0.9 V, which undergoes slow dissociative adsorption in comparison with glyceraldehyde and glycerol. Gomes et al. (2013) explored the effect of glycerol concentration on the main oxidation products during the electrooxidation of glycerol in acidic media over Pt, as analyzed by *in situ* Fourier transform infrared (FTIR) spectroscopy. Based on their results, they suggested that the magnitude of the different oxidation routes depends on the concentration of glycerol and correlates with the nature of the adsorbed species present at the earlier adsorption of glycerol. On the Pt sites, glycerol vies with hydrogen because there is a gradual formation of CO on the surface due to desorption protons from the Pt sites. The concentration of glycerol determines the CO oxidation capacity of the Pt surface. The Pt surface is much more exposed to the adsorbed glycerol residues and inhibits co-adsorption of water at high glycerol concentration. Therefore, there is a delay in water splitting, making it possible for the Pt surface to retain CO at higher potentials. The formation of the CO layer is also favored by the dissociative adsorption of glyceraldehyde, being an intermediate in concentrated glycerol solutions. Moreover, there is a parallel formation of carboxylic acids at intermediate and high potentials, and the carboxylic acid is partly oxidized to  $\text{CO}_2$ .

To use glycerol as a fuel in DAFCs, control of the electrooxidation route is necessary for the improvement of

**Table 1:** Typical oxidation products and their applications.

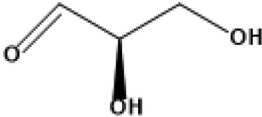

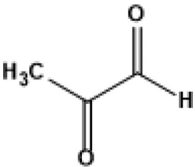
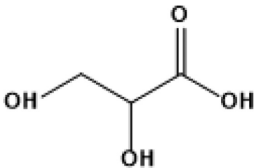
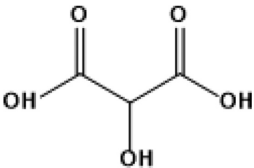
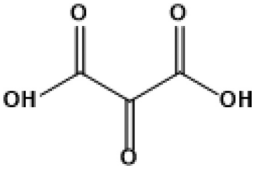
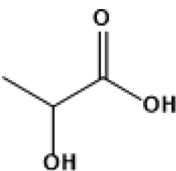
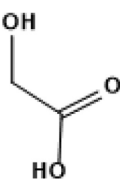
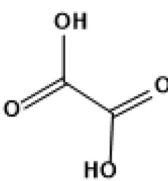
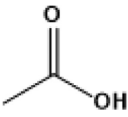
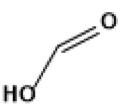
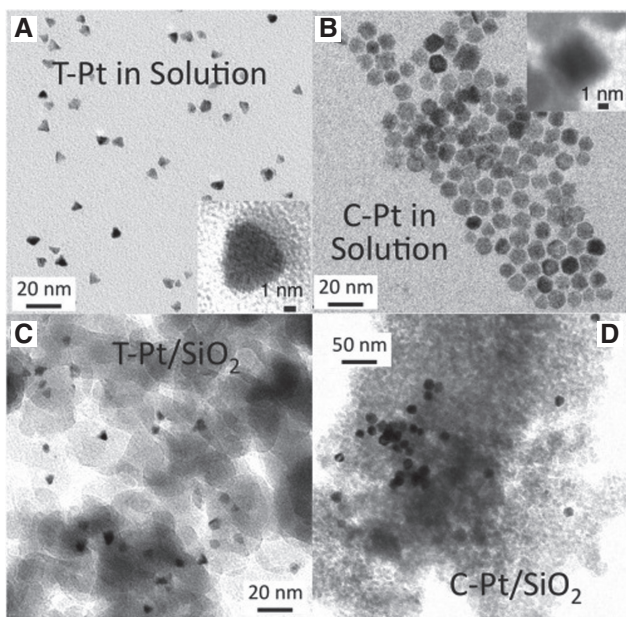
Product	Description	Application	Reference
<p>Glyceraldehyde</p> 	<p>Glyceraldehyde (C<sub>3</sub>H<sub>6</sub>O<sub>3</sub>), also known as glyceral, is a triose monosaccharide, which is the simplest of all common aldoses. It is a colorless and sweet crystalline solid, which could be obtained as an intermediate species during glycerol oxidation</p>	<p>Anti-aging agent, production of advanced glycation end-products (AGEs), fundamental metabolite, modification and cross-linking of proteins</p>	<p>Bijvoet et al. (1951), Pinter et al. (1967)</p>
<p>Dihydroxyacetone</p> 	<p>Dihydroxyacetone (C<sub>3</sub>H<sub>6</sub>O<sub>3</sub>) (DHA), also called glycerone, is a simple saccharide (a triose). It is a ketotriose comprising acetone with hydroxy substituents at 1 and 3 positions. It is the parent of the class of glycerones and the simplest member of the class of ketoses</p>	<p>Antifungal agent, raw material for D,L-serine production, monomer for polymeric biomaterials, metabolite for human, <i>Escherichia coli</i>, and <i>Saccharomyces cerevisiae</i> metabolite, tanning agent in cosmetics, synthon in organic chemistry</p>	<p>Bagheri et al. (2015), Behr et al. (2008), Painter et al. (2010)</p>
<p>Pyruvaldehyde</p> 	<p>Pyruvaldehyde (C<sub>3</sub>H<sub>4</sub>O<sub>2</sub>), also called 2-oxopropanal or methylglyoxal, is the organic compound with two carbonyl groups, a ketone and an aldehyde in gaseous state but in aqueous solution it occurs as oligomers and hydrates. Its conjugate acid is pyruvic acid. Pyruvaldehyde occurs naturally in some kinds of honey such as manuka honey</p>	<p>Marker for investigation of the connection between advanced glycation end products (AGEs) with adverse health outcomes, prevention of <i>S. aureus</i> and <i>E. coli</i>, prevention of <i>P. aeruginosa</i>-produced biofilms</p>	<p>Israili (2014), Loeffler et al. (2006)</p>
<p>Glyceric acid</p> 	<p>Glyceric acid (C<sub>3</sub>H<sub>6</sub>O<sub>4</sub>) is a conjugate acid of glycerate, and a natural three-carbon sugar acid, product of glycerol oxidation. It is a trionic acid, comprising propionic acid substituted at the second and third positions by hydroxy groups</p>	<p>Treatment of skin disorder, intermediate in amino acid synthesis, metabolite in glycolysis cycle, medicine</p>	<p>Behr et al. (2008), Corma et al. (2007), Li and Zaera (2015)</p>
<p>Tartronic acid</p> 	<p>Tartronic acid (C<sub>3</sub>H<sub>4</sub>O<sub>5</sub>), also called 2-hydroxymalonic acid, is a conjugate acid of tartronate and a dicarboxylic acid. It is a malonic acid substituted by a hydroxy group at the second position and its derivative, 2-methyltartronic acid, is an isomalic acid. Tartronic acid is a conjugate acid of a hydroxymalonate and a hydroxymalonate(1-)</p>	<p>Treatment of obesity and osteoporosis, oxygen scavenger</p>	<p>Behr et al. (2008), Hurley (1982), Katryniok et al. (2011)</p>
<p>Mesoxalic acid</p> 	<p>Mesoxalic acid (C<sub>3</sub>H<sub>2</sub>O<sub>5</sub>), also known as ketomalonic acid or oxomalonic acid, is a conjugate acid of mesoxalate. Mesoxalic acid is both a ketonic acid and a dicarboxylic acid, which voluntarily loses two protons to produce mesoxalate, a divalent anion C<sub>3</sub>O<sub>5</sub><sup>2-</sup></p>	<p>Anti-HIV agent, raw material for organic synthesis, complexing agent</p>	<p>Bagheri et al. (2015), Ciriminna and Pagliaro (2003), Johnson and Taconi (2007)</p>



Table 1 (continued)

Product	Description	Application	Reference
<p>Lactic acid</p> 	<p>Lactic acid (C<sub>3</sub>H<sub>6</sub>O<sub>3</sub>) is the conjugate acid of lactate, and an α-hydroxy acid (AHA) because of the existence of a carboxyl group which is adjacent to the OH group. Lactic acid is synthesized conventionally by chemical synthesis or by fermentation of carbohydrates like glucose, lactose, or sucrose</p>	<p>Synthetic intermediate in many organic synthesis industries and in various biochemical industries, food preservative, flavoring agent, and curing agent, decontaminant in meat processing, moisturizer in cosmetics, dyeing agent in textile industry, for making yogurt and cheese production in dairy industry, tanning leather, raw material in pharmaceutical industry, production of inks and lacquers</p>	<p>Abdel-Rahman et al. (2011), Vaidya et al. (2005)</p>
<p>Glycolic acid</p> 	<p>Glycolic acid (C<sub>2</sub>H<sub>4</sub>O<sub>3</sub>), also known as hydroxyacetic acid or hydroacetic acid, is a conjugate acid of glycolate and the smallest α-hydroxy acid (AHA). It is an odorless, hygroscopic, and colorless crystalline solid, which is extremely water-soluble. Glycolic acid is found in some sugar crops</p>	<p>Skin care products, leather tanning agent, decreasing agent, textile dyeing, rust removal, chemical peels performed in dermatology</p>	<p>Bagheri et al. (2015), Sankar et al. (2009)</p>
<p>Oxalic acid</p> 	<p>Oxalic acid (C<sub>2</sub>H<sub>2</sub>O<sub>4</sub>) is a conjugate of oxalate and the simplest dicarboxylic acid. It forms a colorless solution in water since it is a colorless crystalline solid. It is a stronger acid than acetic acid and occurs in various vegetables and plants, and produced in human body by metabolism of ascorbic acid or glyoxylic acid</p>	<p>Cleaning agent, including sterilizing of household articles, rust removal, cleaning of kitchen sinks, bathtubs and counters, detergent and bleach additive, mineral processing mechanisms, bleaching agent in textile industry, purification and dilution of certain chemicals</p>	<p>Önal (2011), Sah and Verma (2011), Simoneit (2004)</p>
<p>Acetic acid</p> 	<p>Acetic acid (CH<sub>3</sub>COOH), also known as ethanoic and methane carboxylic acid, a weak acid, which is the conjugate acid of acetate and the most important synthetic carboxylic acid. In its pure/undiluted form, it is called glacial acetic acid, a colorless liquid with a pungent and strong smell, which characterizes the odor of vinegar</p>	<p>Production of vinegar, antifungals, antibacterials, inhibition of carbohydrate metabolism, synthesis of chemical compounds like vinyl acetate monomer, ester and acetic anhydride, manufacture of perfumes, dyes, and inks, organic compound purification, antiseptic against staphylococci, pseudomonas, streptococci, enterococci, and others, screening of cervical cancer, treatment of outer ear infections</p>	<p>Dibb and Arsenault (2002), Fornaro and Gutz (2003), Staudt et al. (2000)</p>
<p>Formic acid</p> 	<p>Formic acid (HCOOH), also called methanoic acid, is a conjugate of formate ion, a strong electrolyte, a liquid fuel at room temperature, and the simplest form of carboxylic acid. It is an important intermediate in chemical synthesis and could occur naturally, particularly in some ants</p>	<p>Fuel in fuel cells, reducing agent, environmentally benign runway anti-icing (formic acid salts), important intermediate in the synthesis of some organic compounds, finishing, grass silage in Europe, food additive, leather tanning in Asia</p>	<p>Aslam et al. (2012), Behr et al. (2008), Hurley (1982)</p>



**Figure 1:** TEM images of (A) tetrahedral and (B) cuboctahedral platinum nanoparticles, as prepared (top) and after dispersion on a silica support (bottom). High-resolution images of the free (C) tetrahedral (D) and cubic nanoparticles (Li and Zaera 2015). Reproduced with kind permission from Elsevier (copyright license no. 4621250518677).

CO<sub>2</sub> production at low potentials and maximization of the energy delivery to the electrochemical interface (Kwon et al. 2012). To achieve these, good understanding of the role of each superficial site on glycerol electrooxidation is required for the rational design of particular catalysts that favor the anticipated pathways (Fernández et al. 2013). In recent studies where polycrystalline Pt was used, glycerol produces CO<sub>2</sub> from both the terminal carbon and the central one, which suggests that glycerol can dissociate completely on polycrystalline Pt surfaces at least to some extent (Liu et al. 2018b). However, DAFCs require that Pt be applied as NPs (especially with carbon support) in a practical system. However, Pt NPs are far more complex than polycrystalline Pt, primarily because of some factors like the presence of crystalline planes on the same particle as well as low coordination atoms, a wide range of diameters of the particles, different electronic density, etc. (Maillard et al. 2004). Though the study on bulk Pt electrodes is crucial to understanding electrochemical reactions, the outcomes of bulk electrode systems cannot be fully transferred to Pt NPs (Fernández et al. 2013).

The study of Fernández et al. (2013) revealed the fundamentals of the electrooxidation of isotopically labeled glycerol (<sup>13</sup>CH<sub>2</sub>OH-<sup>12</sup>CHOH-<sup>13</sup>CH<sub>2</sub>OH) on the surfaces of carbon-supported Pt NPs. They reported the formation

of glyceraldehyde as an intermediate in glyceric acid production. During the early adsorption steps, FTIR analysis revealed that glycerol could be transformed into CO completely. However, the central carbon (<sup>12</sup>C) is rather protected by its carbon chain, and its oxidation is preceded by the oxidation of the terminal groups (<sup>13</sup>C). CO<sub>2</sub> is produced from both the central and terminal carbons. However, the terminal carbons oxidize more quickly than the central groups, possibly because of the steric effect triggered by <sup>13</sup>CH<sub>2</sub>OH, which hinders <sup>12</sup>CHOH from being oxidized.

Despite the popularity Pt NPs as an electrocatalyst in GEOR, its commercial application is hindered by its exorbitant cost, deactivation at potentials above 0.8 V (Sandrini et al. 2018), low C-C bond cleavage ability, and CO poisoning of Pt active sites due to incomplete oxidation (Caneppele et al. 2017, Ashok et al. 2018). Nevertheless, modification of the Pt surface with adatoms can trigger the production of some commercially valuable compounds via the incomplete oxidation routes. Kwon et al. (2014) reported that GEOR could be enhanced by decorating the Pt/C NPs with Sb, Sn, In, Bi, and Pb. Functionalization of Pt/C NPs with Sb or Bi not only improves GEOR but also redirects the reaction toward DHA formation, with 100% selectivity achieved using Bi (Kwon et al. 2012, 2014). Lee et al. (2016) reported remarkable yield and selectivity of DHA using PtSb/C in acidic media, achieving 61% yield and 90% glycerol conversion. They suggested that the DHA selectivity could be enhanced by carefully increasing the potential. However, there is formation of C<sub>1</sub> and C<sub>2</sub> products at higher anode potentials, which favors C-C cleavage. Caneppele et al. (2017) explored the effect of the degree of Sb coverage on the surface of Pt/C NPs in GEOR. They reported an exponential enhancement in catalytic performance up to Sb=0.81. The Sb atoms were stable on the surface of Pt NPs except for potentials ≥0.70 V.

The surface structure of the Pt electrode plays a vital role in GEOR and its selectivity. While the surface structure of Pt(111) is selective toward primary and secondary alcohol, the surface structure of Pt(100) is selective only toward primary OH group (Garcia et al. 2016). The above claims stand even if the electrode is modified. The reports of Garcia et al. (2015) and Zalineeve et al. (2014) using Bi-modified Pt electrodes reveal that modification of Pt(111) with Bi increases the concentration of glyceraldehyde (primary OH groups) and dihydroxyacetone (secondary OH groups), while modification of Pt(100) enhances the concentrations of glyceric acid and glyceraldehyde in comparison with the parent Pt(100) surface (Table 2).

Moreover, Pt can be fortified by incorporating supports such as SiO, CeO<sub>2-x</sub>, graphene oxide (GO), etc., which can ease electron transfer and enable facile transfer of target



**Table 2:** Typical catalysts and product distributions for GEOR on Pt-based catalysts.

Catalyst	GLY/Cat (mol:mol)	Anode potential (V)/ membrane	Electrolyte formulation	Conv. (%)/ time (h)	Selectivity (%)					References	
					TA	GLA	DHA	GLAD	MOXA		GLCA
Pt/C		0.5 V (vs. SHE)/AEM A201	2.0 M KOH + 1.0 M glycerol, 60°C	10.5/2	40	41			0	4	Zhang et al. (2012d)
				16.2/4	39	44			0	4	
				20.4/6	38	45			0	5	
				21.5/2	33	44			2	5	
				4.4/2	37	47			0	16	
Pt/GNS		0.5 V (vs. SHE)/AEM A201	4.0 M KOH + 1.0 M glycerol, 60°C	10.7/2	45	41			1	5	
				3.1/2	33	38			0	15	
				-2	0.01	4.78	8.83		8.88	Chen et al. (2019)	
				-2	0.08	5.92	4.50		14.32		
				-2	0.17	5.74	2.66		18.63		
Pt-CeO <sub>2</sub> x/GNS		0.5 V (vs. SCE)/Nafion 112	0.5 M KOH + 0.5 M glycerol, 20 ml	-2	0.02	4.30	9.47		0.40		
				-2	0.01	6.30	7.85		2.40		
				-2	0	2.52	9.17		0.15		
				73.6	5.91			1.68			
				68.3	14.0			3.42			
Pt/C		0.726 V (vs. RHE)/PBI	4.0 M KOH + 1.0 M glycerol, 60°C	10.5/10	25.4	25.4	73.0		2.61	Kim et al. (2017)	
				35.4/10	25.6	20	65.6		11.1		
				68.0/10	50.0	8.91	37.9		12.3		
				5.2/10	0		100		0		
				16/10	11.5	5.23	85.6		2.93		
Pt/C		0.726 V (vs. RHE)/PBI	4.0 M KOH + 1.0 M glycerol, 90°C	37.7/10	21.7	21.7	74.9		2.20		
				12.4/10	32.8	32.8	74.5		0		
				30.2/10	78.8	78.8	31.1		0		
				43.5/10	83.4	83.4	13.0		0		
				90/10	90.1	90.1	2.89		0.48		
Pt(100)/Birr		0.9 (vs. SHE)/PEM	0.5 M H <sub>2</sub> SO <sub>4</sub> + 1.0 M glycerol, 60°C	64.1/10	1.3	67.3	20.0		0	3.7	
				67.2/10	1.7	46.0	34.2		5.4	9.6	Garcia et al. (2017)
				0.9 (vs. RHE)/-			11.2		65.8		
				0.9 (vs. RHE)/-			33.6		51.9		
				0.83 (vs. RHE)/-			37.6		51.9		
Pt(100)/Birr		0.77 (vs. RHE)/-	0.5 M HClO <sub>4</sub> + 0.1 M glycerol, 20°C	23.3	43.4	40.3					
				0.7 (vs. RHE)/-	25.5	37.6	43.9				
				0.65 (vs. RHE)/-	36.3	34.9	63.1				
				0.6 (vs. RHE)/-	0	31.3	79.3				

Table 2 (continued)

Catalyst	GLY/Cat (mol: mol)	Anode potential (V)/ membrane	Electrolyte formulation	Conv. (%)/ time (h)	Selectivity (%)							References		
					TA	GLA	DHA	GLAD	MOXA	GLCA	HPA			
Pt/C		0.9 (vs. RHE)/-	0.5 M H <sub>2</sub> SO <sub>4</sub> + 0.1 M glycerol		7.63								97.7	Kwon et al. (2012)
		0.83 (vs. RHE)/-			6.76								98.2	
		0.77 (vs. RHE)/-			10.4								95.1	
		0.7 (vs. RHE)/-			11.3								94.3	
		0.65 (vs. RHE)/-			8.63								96.5	
		0.43 (vs. RHE)/-			9.3	0.76							90.8	
		0.67 (vs. RHE)/-			18.4	1.01							80.8	
		0.9 (vs. RHE)/-			23.7	62.0							75.3	
		0.43 (vs. RHE)/-				80.0							38.3	
		0.48 (vs. RHE)/-			3.66	60.5							17.4	
Pt/C in Bi saturated solution		0.67 (vs. RHE)/-			13.4	60.5							26.1	
		0.9 (vs. RHE)/-			24.8	7.09							68.9	
		0.43 (vs. RHE)/-			9.49	82.2							96.5	
		0.67 (vs. RHE)/-			17.2	59.6							23.8	
PtSb/C		0.797 (vs. SHE)/-/Nafion	0.5 M H <sub>2</sub> SO <sub>4</sub> + 0.1 M glycerol, 10 ml, 60°C		46.0/-								13.0	Lee et al. (2016)
		50/-			0.6	86.8								
		75.5/-			1.3	81.2						11		
		90.3/-			1.86	79.9						16.2		
		50/-			7.86	68.5						19.1		
PtBi/C					18.3	11.1						40.2		
					50/-	18.4	1.3							58.7

GLA, glyceric acid; TA, tarttronic acid; DHA, dihydroxyacetone; GLAD, glyceraldehyde; GLCA, glycolic acid; MOXA, mesoxalic acid; PBI, polybenzimidazole membrane.

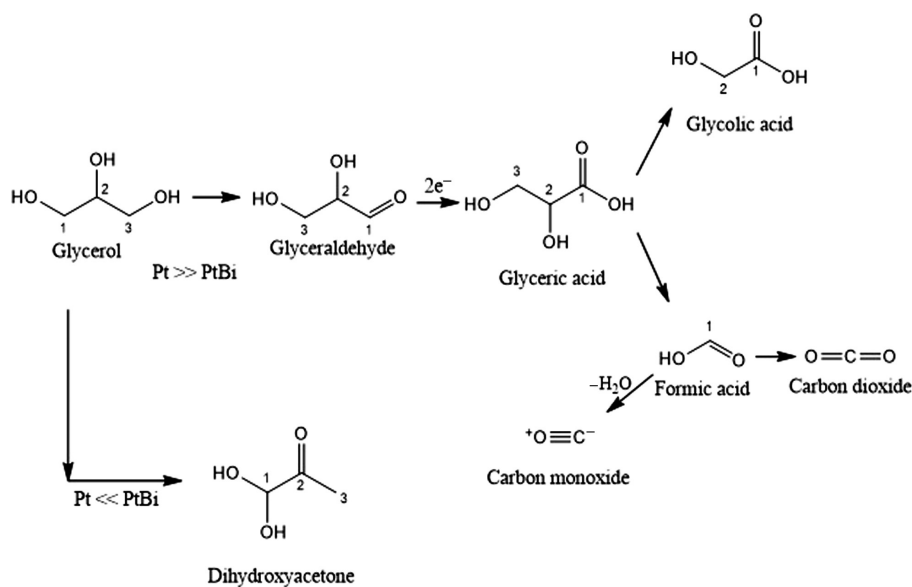
analytes at the surface of the electrode to enhance the catalytic performance, particularly product selectivity (Rezaei et al. 2014). This fortification will help in reducing the amount of metal loading as well as enhancing their stability, electrocatalytic activity, and utilization efficiency. For instance, Zhang et al. (2017b) achieved 85.9% GLA selectivity using PtCo/RGO catalyst, which is higher than that of Co/RGO and Pt/RGO. Zhang and Shen (2015) and He et al. (2016) developed a three-component hybrid catalyst comprising ultrafine Pt nanoparticles incorporated on graphene nanosheets fortified with ceria (Pt-CeO<sub>2-x</sub>/GNS). The catalyst exhibited remarkable performance toward the electrooxidation of alcohol. Recently, Chen et al. (2019) used the catalyst to study GEOR. They observed that the catalyst favors the production of C3 products with 52% selectivity of glyceraldehyde (GALD) at a potential of -0.4 V. Pt-CeO<sub>2-x</sub>/GNS showed improved catalytic activity and durability when compared to Pt/GNS catalyst due to the electronic and bifunctional effects, which enabled the synergistic effects of the constituents. Scheme 2 shows a typical reaction mechanism for the selective oxidation of glycerol over a Pt-based electrocatalyst. Moreover, it is worth mentioning the recent contribution of Wang et al. (2018), where they fabricated amorphous ultra-dispersed Pt clusters supported on carbonized 1,10-phenanthroline-modified carbon (PMC) to form AU-Pt/PMC and Vulcan XC-72R carbon black to form AU-Pt/C for glycerol oxidation. The AU-Pt/PMC catalyst showed superior activity (5.1 times) and stability (24.3 times) when compared with the conventional Pt/C catalyst during the electrooxidation of glycerol. The remarkable performance of AU-Pt/

PMC is traceable to the formation of its unique amorphous ultradispersed structure, and the superimposition of strong metal-support interactions and Pt clusters.

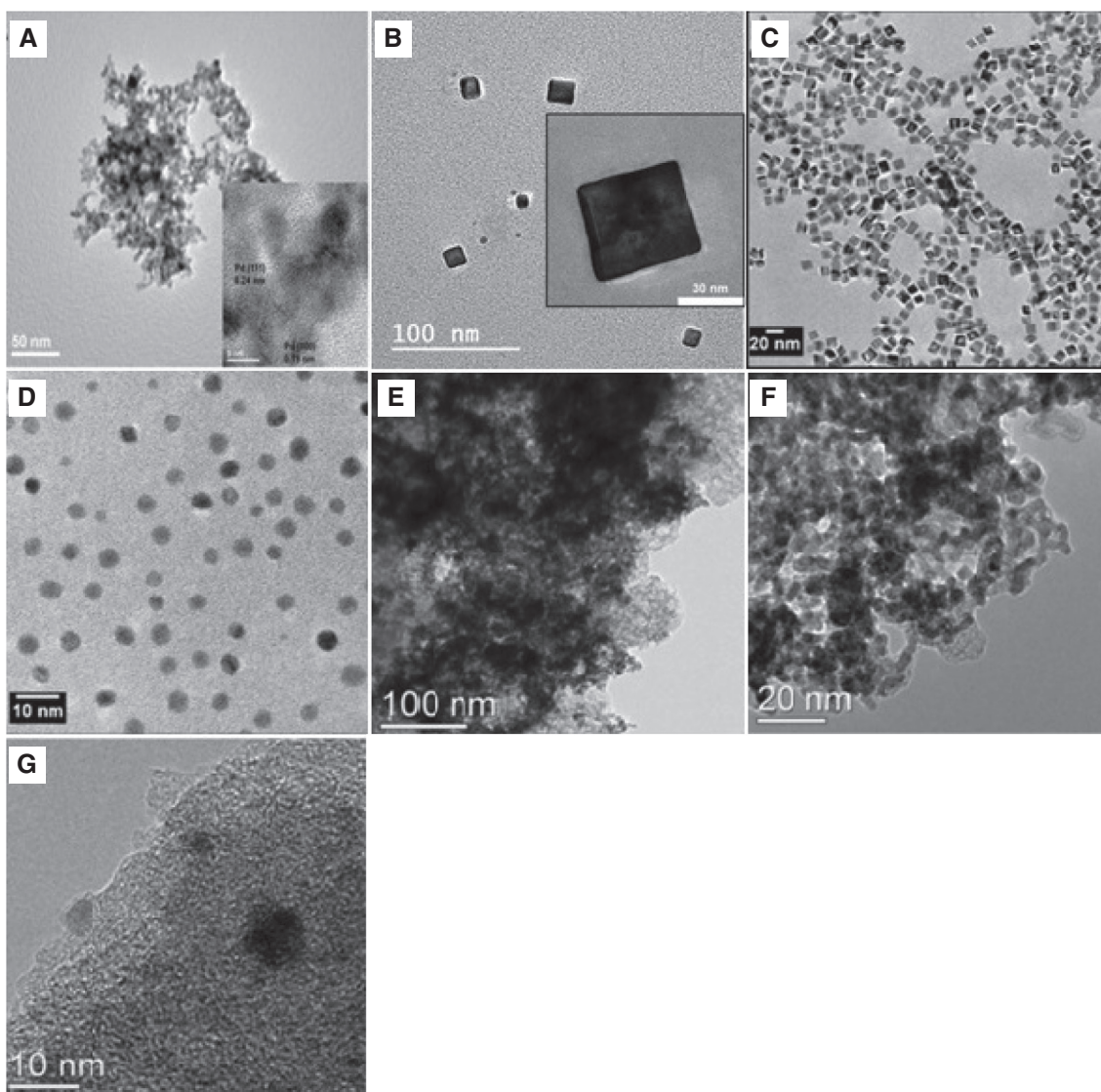
### 3.2 Palladium-based electrocatalysts

Pd-based electrocatalysts are plausible substitutes for Pt-based catalysts since Pd is less expensive and at least 50 times more abundant on earth than Pt (Lee et al. 2016). Several researchers have considered Pd as a metal-base electrocatalyst for energy conversion and production of carbonyl species in fuel cell systems in alkaline solution, suggesting that Pd is a better electrocatalyst (Zhang and Shen 2013, Zalineeve et al. 2015a). The electrochemical performance of Pd largely depends on its structure (Jin et al. 2011). Moreover, the performance as well as product distribution of Pd electrocatalysts can be tuned by modifying with adatoms (p-group atoms) such as Sn, Bi, and Sb (Simões et al. 2011, Cai et al. 2013). Several authors have reported the remarkable performance of adatoms as a co-catalyst in alcohol oxidation reactions in both acidic and alkaline media (Awasthi and Singh 2012, Ramulifho et al. 2013).

Zalineeve et al. (2013, 2014) developed a self-supported, hierarchical, mesoporous, Bi-modified Pd nanocube {100} surface of nanodomains for glycerol electrooxidation (Figure 2C, D). They reported that the unmodified Pd nanocubes performed better than nanospheres toward GEOR. The enhanced performance by Bi adatoms is aggravated with the Pd nanocubes when compared with



**Scheme 2:** Reaction pathway of the selective oxidation of glycerol over Pt-based electrocatalyst (Kwon et al. 2012). Reproduced with kind permission from the American Chemical Society.



**Figure 2:** TEM images of (A) pure Pd NPs (adopted from Hu and Wang 2015). (B) Pd nanocubes (adopted from Guima et al. 2017); (C, D) Pd nanocubes modified by Bi (adopted from Zalineeva et al. 2013); (E) Pd/Mo<sub>2</sub>C; and (F, G) Pd/WC-Mo<sub>2</sub>C (Zhang and Shen 2013). Reproduced with kind permission from Elsevier (copyright license nos. 4621260132205, 4621261198350, 4621251304727).

the nanospheres. The mechanism of GEOR is influenced by Bi coverage and glycerol concentration, thereby favoring different selective reaction pathways (intermediates). CO<sub>2</sub> is formed at high potentials and hydroxypyruvate at moderate potentials, and ketone and aldehyde are produced at low potentials, indicating that product distribution solely depends on the anode potential (Zalineeva et al. 2014). In the presence of Bi, there is co-adsorption of OH<sup>-</sup> with Bi, indicating that Bi supports OH species adsorption either on adjacent noble metal sites (Schmidt et al. 2000) or on its surface (Zalineeva et al. 2015b). Like Bi, Sn has been investigated in the preparation of self-supported hierarchical nanoporous Pd<sub>1</sub>Sn<sub>x</sub> for GEOR. Zalineeva et al. (2015b) fabricated Pd<sub>1</sub>Sn<sub>x</sub> using a sacrificial support method (SSM).

Their results revealed that modification with Sn suppresses the glycerol dissociative adsorption process with C-C bond breakage and supports the bifunctional mechanism. The oxophilic nature of Sn atoms at the surface of Pd<sub>1</sub>Sn<sub>x</sub> enables the complete shifting of selectivity toward carboxylate species production at the start of the oxidation onset potential at low anode potential. The unique catalytic performance of self-supported adatom-modified Pd is ascribed to its morphology and structure. To further enhance the performance of PdSn, Wang et al. (2016) incorporated functionalized carbon (phen-C) support using phenanthroline. They reported that a rationally designed PdSn alloy supported on carbon modified with phenanthroline exhibited enhanced electroactive surface

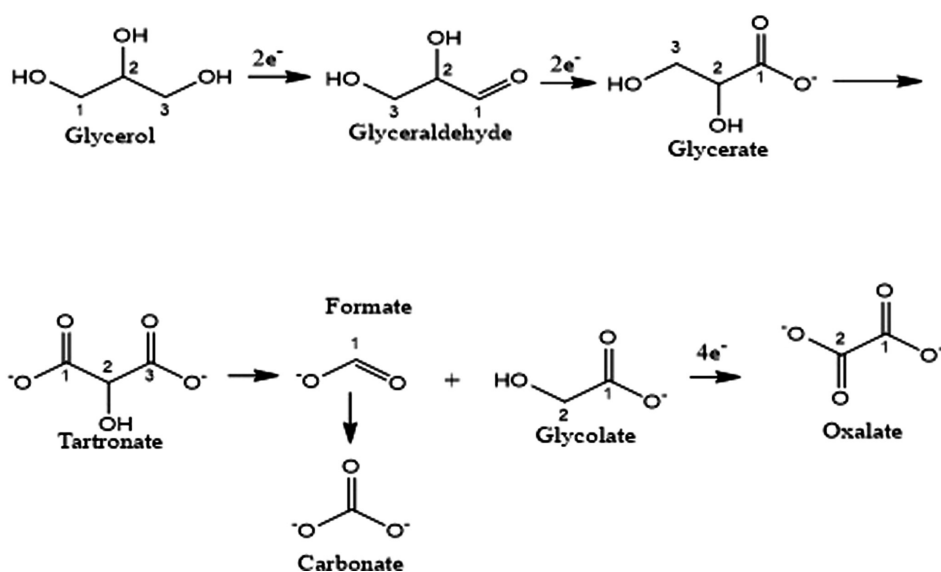
area, durability, and poison tolerance, traceable to the distinct conjunct effects between phen-C and PdSn.

Several studies have revealed that Pd with metal oxides such as  $\text{CeO}_2$ ,  $\text{TiO}_2$ ,  $\text{Mn}_3\text{O}_4$ ,  $\text{Co}_3\text{O}_4$ , and NiO electrocatalysts is promising toward the electrooxidation of alcohols in alkaline electrolytes (Xu et al. 2008). Su et al. (2009) developed Pd-supported titanium dioxide (Pd/ $\text{TiO}_2$ ) nanofibers and used them for GEOR in an alkaline solution. They reported remarkable electrocatalytic performance of Pd/ $\text{TiO}_2$  over GEOR. The concentrations of both glycerol and KOH influence glycerol electrooxidation based on the current densities of the forward and backward scan peak and peak potential. Simões et al. (2010) proposed replacing 50% of the Pd species with Ni species to boost the catalytic performance, thereby decreasing the cost of the catalyst. Zhiani et al. (2013) fabricated bis(dibenzylidene acetone)-promoted Pd(0) catalyst ( $\text{Pd}(\text{DBA})_2$ ) for GEOR in an alkaline direct glucose fuel cell (DGFC) and an alkaline half-cell. They reported that the synthesized Pd ( $\text{DBA})_2$  exhibited a remarkable onset potential and specific peak current density, making it a promising anode catalyst for alkaline DGFC.

Pd can also be fortified with other supports such as nanoporous stainless steel (NPSS), carbon aerogel composites (Zhang and Shen 2013), carbon black, multiwalled carbon nanotubes (MWCTs) (Fernández et al. 2012a), graphene (Kim et al. 2011b), nanocrystalline metal oxides (Xu et al. 2008), and  $\text{Co}(\text{OH})_2$  thin films (Das and Das 2010). NPSS-supported Pd electrocatalyst could be achieved using an anodization process, which involves electrodeposition of Cu into the pores of NPSS

and subsequent galvanic replacement to replace the Cu with Pd since noble metals cannot be directly deposited on NPSS (Rezaei et al. 2014). The presence of Cu and the porosity of NPSS enable a highly electrochemically active surface area (EASA), thereby improving the durability of the catalyst and making it suitable for GEOR. From the report of Zhang and Shen (2013) and Hu and Wang (2015), carbon aerogel composites and binary-carbide-supported Pd nanoparticles ( $\text{Pd}@WC\text{-Mo}_2\text{C}/\text{C}$ ) could be synthesized by polycondensing formaldehyde and resorcinol in the presence of sodium molybdate and sodium tungstate. They reported that  $\text{Pd}@WC\text{-Mo}_2\text{C}/\text{C}$  exhibits better electrocatalytic activity toward GEOR than Pd/C based on the peak current density. The peak current density of  $\text{Pd}@WC\text{-Mo}_2\text{C}/\text{C}$  is about 2 times higher than that of Pd/C.  $\text{Pd}@WC\text{-Mo}_2\text{C}/\text{C}$  also exhibits superior resistance to CO poisoning when compared with Pd/C. The remarkable performance of  $\text{Pd}@WC\text{-Mo}_2\text{C}$  is traceable to the modified structure (three-dimensional structure) and porosity of the catalysts (Figure 2E–G). Hu and Wang (2015) and Zhang and Shen (2013) prepared Pd NPs supported on commercial carbon black (Pd/CB). The sample was prepared using a novel route without using a surfactant and a cumbersome heating process. They reported that Pd/CB exhibited ultra-high electrocatalytic performance, remarkable long-term stability, and fantastic electrical conductivity, making it suitable for GEOR. Scheme 3 shows a typical reaction mechanism for the selective oxidation of glycerol over Pd-based electrocatalyst in an alkaline electrolyte.

Table 3 presents the performance parameters of some Pd-based catalysts during GEOR. The catalytic



**Scheme 3:** GEOR mechanism on Pd surface in alkaline electrolyte (adapted from Guima et al. 2017). Reproduced with kind permission from American Chemical Society.

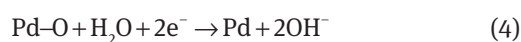


**Table 3:** Performance parameters of some Pd-based electrodes for GEOR.

Electrode composition	Electrolyte	Pd loading ( $\mu\text{g cm}^{-2}$ )	$E_{\text{onset}}$ (V)	$E_p$ (V)	$J_p$ ( $\text{mA cm}^{-2}$ )	$J_s$ ( $\text{mA } \mu\text{g}_{\text{Pd}}^{-1}$ )	References
Pd/carbon/GCE	1 M NaOH+0.1 M GLY	145	0.55	0.85 (vs. RHE)	25	0.17	Simões et al. (2010)
Pd0.5Au0.5/C/GCE	1 M NaOH+0.1 M GLY	65	0.45	0.88 (vs. RHE)	33	0.09	Simões et al. (2010)
Pd nanocubes	0.1 M KOH+0.2 M GLY	160	-0.66	0.87 (vs. RHE)	2.5	-	Guima et al. (2017)
Pd/CPAA	1 M KOH+1 M GLY	300	-0.3	-0.1 (vs. Hg/HgO)	70	0.23	Wang et al. (2006)
Pd(DBA) <sub>2</sub>	2 M KOH+1 M GLY	30	-0.33	0.08 (vs. NHE)	16	0.48	Zhiani et al. (2013)
Pd/carbon ceramic/Gr	0.3 M NaOH+0.5 M GLY	500	-0.21	0.16 (vs. SCE)	51.8	0.10	Habibi and Razmi (2012)
Pd/C	1 M NaOH+1 M GLY			0.7 (vs. SCE)	2.49	1.21	Hu and Wang (2015), Zhang and Shen (2013)
Pd/CB	0.1 M NaOH+0.1 M GLY			0.7 (vs. SCE)	1.91	2.39	Hu and Wang (2015), Zhang and Shen (2013)
Pd/carbon black/Gr	1 M KOH+1 M GLY	300	-0.15	0.23 (vs. Hg/HgO)	18	0.06	Xu et al. (2008)
Pd <sub>2</sub> (Mn <sub>3</sub> O <sub>7</sub> )/carbon black/Gr	1 M KOH+1 M GLY	300	-0.25	0.16 (vs. Hg/HgO)	65	0.22	Xu et al. (2008)
Pd <sub>2</sub> (Co <sub>3</sub> O <sub>7</sub> )/carbon black/Gr	1 M KOH+1 M GLY	300	-0.24	0.09 (vs. Hg/HgO)	70	0.23	Xu et al. (2008)
Pd <sub>4</sub> (NiO)/carbon black/Gr	1 M KOH+1 M GLY	300	-0.18	0.11 (vs. Hg/HgO)	88	0.29	Xu et al. (2008)
Pd <sub>1.3</sub> (CeO <sub>2</sub> )/carbon black/Gr	1 M KOH+1 M GLY	300	-0.19	0.09 (vs. Hg/HgO)	50	0.17	Xu et al. (2008)
Pd	1 M KOH+0.1 M GLY	200		0.87 (vs. RHE)	21	0.11	Zalineeva et al. (2014)
Pd <sub>2</sub> Bi	1 M KOH+0.1 M GLY	200		0.97 (vs. RHE)	48.3	0.34	Zalineeva et al. (2014)
Pd <sub>4</sub> Bi	1 M KOH+0.1 M GLY	200		1.07 (vs. RHE)	90.3	0.54	Zalineeva et al. (2014)
Pd <sub>6</sub> Bi	1 M KOH+0.1 M GLY	200		0.95 (vs. RHE)	61.2	0.35	Zalineeva et al. (2014)
Pd/CPAA/Gr	1 M KOH+1 M GLY	300	-0.32	-0.06	72	0.24	Wang et al. (2006)
Pd/CNT-FLG/GCE	2 M KOH+10 wt% GLY	24-30	0.57	0.92 (vs. RHE)	44.2-55.2	1.84	Machado et al. (2013)
Pd/MWCNT/GCE	2 M KOH+5 wt% GLY	17	-0.40	0.12 (vs. Ag/AgCl)	53.7	2.80	Bambagioni et al. (2009)
Commercial Pd black	0.5 M KOH+0.5 wt% GLY	17	-0.45	0.003 (vs. SCE)	-	0.023	Li et al. (2014)
10% Pd/C	0.5 M KOH+0.5 wt% GLY	17	-0.40	-0.12 (vs. SCE)	-	0.004	Li et al. (2014)
Pd/RGO	0.5 M KOH+0.5 wt% GLY	17	-0.46	-0.12 (vs. SCE)	-	0.025	Li et al. (2014)
Pd/NPSS	1 M KOH+5 wt% GLY	11	-0.32	0.1	78	0.0027	Rezaei et al. (2016)
Pd/NPSS	1 M KOH+5 wt% GLY	243	-0.25	0.04 (vs. Ag/AgCl)	5.3	0.02	Rezaei et al. (2014)
Pd/Cu/NPSS	1 M KOH+5 wt% GLY	29	-0.35	0.04 (vs. Ag/AgCl)	23.8	0.82	Rezaei et al. (2014)
PdSn/phen-C	0.1 M KOH+0.5 wt% GLY	20 wt%		-0.1 (vs. Ag/AgCl)		0.0073	Wang et al. (2016)
Pd <sub>2</sub> Sn <sub>3</sub> phen-C	0.1 M KOH+0.5 wt% GLY	20 wt%		-0.1 (vs. Ag/AgCl)		0.0054	Wang et al. (2016)
Pd <sub>3</sub> Sn/phen-C	0.1 M KOH+0.5 wt% GLY	20 wt%		-0.1 (vs. Ag/AgCl)		0.0132	Wang et al. (2016)
Pd/phen-C	0.1 M KOH+0.5 wt% GLY	20 wt%		-0.1 (vs. Ag/AgCl)		0.0108	Wang et al. (2016)
Pd/C	0.1 M KOH+0.5 wt% GLY	20 wt%		-0.1 (vs. Ag/AgCl)		0.0089	Wang et al. (2016)
Pd-CB	0.5 M KOH+0.5 wt% GLY	24.55 wt%		0.332 (vs. Hg/HgO)		0.907	Wang et al. (2015)
Pd-CN <sub>x</sub>	0.5 M KOH+0.5 wt% GLY	26.35 wt%		0.354 (vs. Hg/HgO)		1.07	Wang et al. (2015)
Pd-CN <sub>x</sub> /G	0.5 M KOH+0.5 wt% GLY	23.93 wt%		0.347 (vs. Hg/HgO)		1.12	Wang et al. (2015)
Pd/CCE	0.3 M KOH+0.5 M GLY	500	-0.45	-0.085 (vs. SCE)	51.8	-	Habibi and Razmi (2012)
PdRh/ED	0.1 M KOH+0.1 M GLY			0.91 (vs. RHE)	1.16	-	Ferreira Jr et al. (2013)

GCE, glassy carbon; Gr, graphite; CPAA, carbonized and pulverized porous anodic alumina; CNT-FLG, nanotube-graphene composite; CCE, carbon ceramic electrode; CB, carbon black; NPSS, nanoporous stainless steel;  $E_p$ , forward peak potential;  $E_{\text{onset}}$ , forward peak potential;  $E_s$ , sweep rate: 10 mV s<sup>-1</sup>;  $J_p$ , mass activity;  $J_s$ , specific activity;  $J_p = J_s/\text{ECSA}$ ; PdRh/ED, electrodeposit of PdRh prepared by electrochemical reduction of Pd<sup>2+</sup> and Rh<sup>3+</sup>.

performance depends on the onset potential, anodic peak potential, ECSA, forward anodic peak current density, and the ratio of forward anodic peak current density ( $\text{mA mg}^{-1}$ ) to reverse anodic peak current density. Lower onset potential, higher ECSA, and a higher ratio of the forward to reverse anodic peak current density indicate higher catalytic activity (Li et al. 2014). Furthermore, a higher ratio of forward to reverse anodic peak current density indicates higher catalytic activity due to lower deposition of intermediate carbonaceous residues such as CO and formic acid. This means that more intermediate carbonaceous matter was oxidized to  $\text{CO}_2$  on the surface of the Pd-based electrode (Zhang et al. 2006, Chowdhury et al. 2016). The reverse peak indicates the creation of Pd from Pd-O as shown below:



### 3.3 Gold-based electrocatalysts

The prohibitive cost and scarcity of catalysts based on Pd and Pt NPs have called for the search for suitable alternatives. One of the promising alternative catalysts in this regard is Au NPs. Several researchers have used Au as an electrooxidation catalyst for borohydride, glucose, methanol, and isopropanol in alkaline media (Guerra-Balcázar et al. 2010, Santos and Sequeira 2010, Wang et al. 2019). In particular, a few authors have investigated the performance of Au in GEOR (Jeffery and Camara 2010, Kwon et al. 2011a). Moreover, some authors have investigated Au and Pt as catalysts for GEOR in alkaline electrolytes. Roquet et al. (1994) and Simões et al. (2010) reported that Au is more efficient in promoting GEOR because, unlike Pt, Au is not susceptible to surface poisoning by CO; CO rather promotes glycerol oxidation on Au-based catalysts (Zhang et al. 2016a). Furthermore, Au can adsorb an OH monolayer, which facilitates any oxidation reaction. Simões et al. (2010) explored GEOR using Au NPs supported on carbon. The spectroscopic results were compared with those observed for Pt- and Pd-based catalysts, and the authors observed that the hydroxypyruvate ion was formed only on Au NPs. Other compounds studied by the authors included glyceraldehyde, tartronate, glycerate, mesoxalate, and 1,3-dihydroxy-2-propanone (Simões et al. 2010).

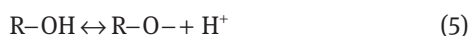
Jeffery and Camara (2010) explored the performance of polycrystalline Au in alkaline media on GEOR. By using *in situ* FTIR during a voltammetric scan, the observed products included  $\text{CO}_2$ , hydroxypyruvate, glycerate, glycolate, formate, carbonate, and glyceraldehyde. They

attributed the formation of  $\text{CO}_2$  to a sudden decline in pH stimulated by  $\text{OH}^-$  consumption, thereby forcing some of the reactor content to interact with water to form  $\text{CO}_2$ . Moreover, the Au electrode could perform better than Pt and Pd electrodes based on stability and activity during GEOR. This was confirmed by Zhang et al. (2012a), who showed that the Au electrode was more stable during glycerol and methanol oxidation than the Pt electrode. They also found that the stability and activity of the Au electrode were higher than those of the Pd electrode during glycerol oxidation. Therefore, it is reasonable to conclude that the pH of the working medium and the catalyst's nature predominantly influence both the reaction kinetics and selectivity in GEOR (Carretin et al. 2002). This effect could be elucidated by studying the electrooxidation of different alcohols containing chains with three carbon atoms. Jin et al. (2012) explored the electrooxidation of propane-1,2-diol, glycerol, 1-propanol, and propane-1,3-diol in an alkaline electrolyte under similar conditions on Pt and Au. Their report revealed a great difference based on current densities and ascribed it to the position and number of OH groups in the carbon chain. Nevertheless, the influence of the number and location of OH groups in the molecules on their reaction mechanisms and pathway remains unclear. Recently, De Souza et al. (2017) explored the influence of the number of OH groups and their locations in the carbon chain on their catalytic performance and product distribution, considering oxidation of glycerol, 1-propanol, propane-1,3-diol 2-propanol, and propane-1,2-diol in an alkaline electrolyte. They reported that the reactivity of the alcohols on Au decreased in the following order: 2-propanol  $\approx$  1-propanol < propane-1,3-diol << propane-1,2-diol < glycerol. The product distributions of propane-1,2-diol and glycerol show high rates of C-C bond breakage, as proved by the formation of compounds containing chains with one and two carbon atoms. Meanwhile, only products containing chains with three carbon atoms are observed for the electrooxidation of propane-1,3-diol, 1-propanol, and 2-propanol. Based on their results, they suggested that the existence of vicinal OH groups in the alcohol molecule is an important feature for the breakage of the C-C bond in alkaline media, resulting in further oxidation of products, which subsequently yield more electrons per alcohol molecule and thus higher current densities.

High selectivity towards tartronate is also possible on Au-based catalysts. This is achievable by the rational optimization of the anode potential together with the membrane electrode assembly (MEA) structure, operation temperature, electrolyte pH, and flow rate of the fuel. By doing so, cleavage of the C-C bond to oxalate and

glycolate and overoxidation of the secondary OH to mesoxalate will be minimized, while tartronate formation via electrooxidation of two primary OH groups of glycerol will be favored. Qi et al. (2014) achieved this at <0.45 V anode potential, yielding about 61.8% tartronate from GEOR on Au/C and Au/C nanocapsule anode using an anion electrode membrane fuel cell (AEMFC). The partially oxidized products, including tartronate, glycerate, and mesoxalate, are comparatively stable after desorption into the bulk of the electrolyte. This report was further supported by using half-cell experimental catalysts in an AEM DGFC.

Generally, it is conceivable that Au exhibits low activity for the oxidation of organics at low pH. An *in situ* FTIR spectroelectrochemical study by Gomes and Tremiliosi-Filho (2011) for GEOR on Au in sulfuric acid medium revealed that the adsorption of bisulfate and sulfate anions affected both the spectral analysis and reaction process because of their strong signal. Moreover, an electrochemical analysis was also performed in neutral and acidic media for comparison. Their results revealed that glycerol exhibited much lower current densities in neutral and acidic media compared to alkaline media. This is attributable to the blockage of the surface by  $\text{ClO}_4^-$  anions and the absence of alkoxide (active species in alkaline electrolytes) in neutral and acidic media (De Souza et al. 2017). The alkoxide in the form of Brønsted bases shifts the equilibrium of



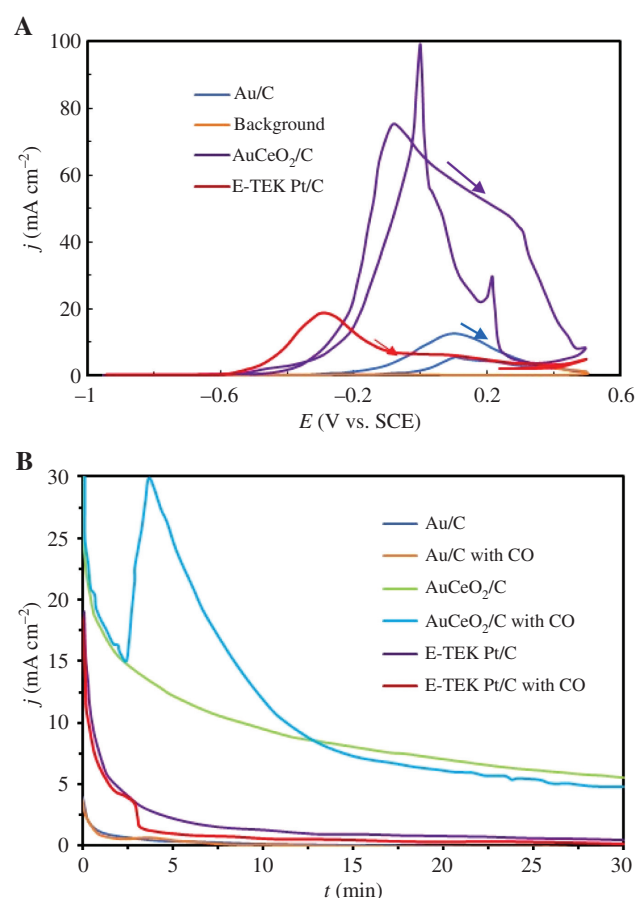
to the right to promote GEOR since the alkoxide is more active than its parent alcohol (Valter et al. 2018).

Valter et al. (2018) studied GEOR on Au in an acidic solution using cyclic voltammetry and density functional theory calculations. The experiment was carried out at a potential above 0.5 V vs. the reversible hydrogen electrode (RHE). The computational study revealed the formation of glyceraldehyde, 2,3-dihydroxy-2-propenal, and dihydroxyacetone at 0.60, 0.39, and 0.39 V vs. RHE, respectively, from partial oxidation of glycerol, while carbon monoxide was formed because of the complete oxidation at 0.50 V vs. RHE. They found that the experimental results agreed with the computational results, indicating that Au is a promising catalyst to produce speciality chemicals and hydrogen.

As mentioned earlier, CO promotes Au-based electrodes rather than poisoning them. For instance, CO promotes a current from 7.5 to 15.0  $\text{mA cm}^{-2}$  on the Au-CeO<sub>2</sub>/C electrode but upon desorption of the CO, the current declines slowly to 7.5  $\text{mA cm}^{-2}$  during GEOR in an alkaline solution (Zhang et al. 2016a). This shows that Au-based

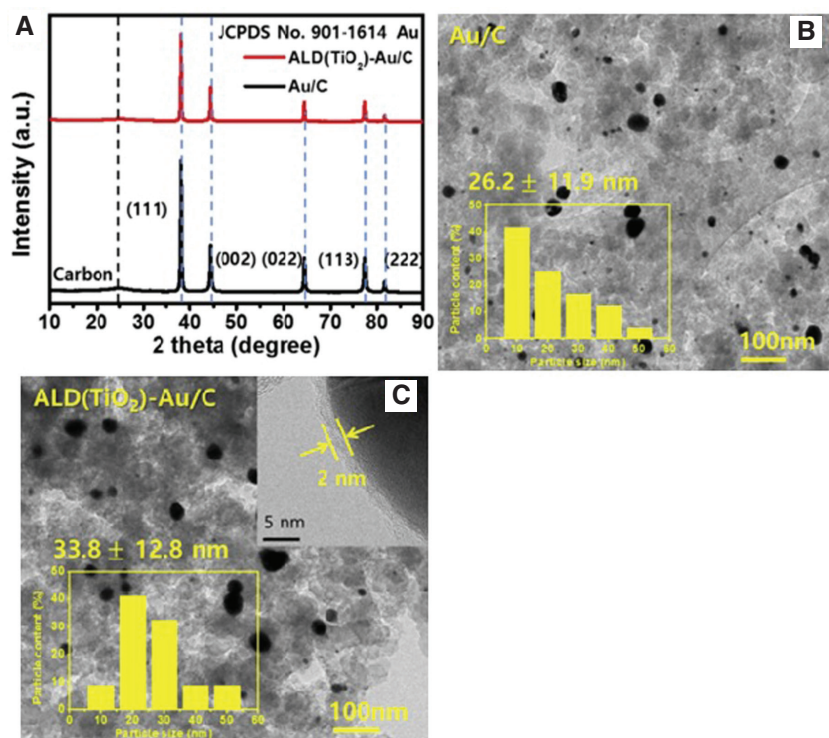
electrodes exhibit superior stability when compared to E-TEK Pt/C during GEOR. Figure 3 shows the chronoamperometric curves for GEOR on Au-based and E-TEK Pt/C electrodes in 1.0 mol l<sup>-1</sup> KOH electrolyte.

Therefore, Au is a promising electrocatalyst for GEOR, displaying orders of magnitude higher performance relative to Pt, due to the higher anodic potential of Au oxidation (Cortright et al. 2011, Kwon et al. 2011a). Meanwhile, the activity of Au in acidic solutions is weak because of the lack of proton acceptors OH<sup>-</sup> in the solution as well as surface-bonded hydroxo adsorbates (\*OH) (Kwon et al. 2011a,b). Moreover, the performance of Au-based catalyst can be enhanced by modifying it with metal oxides without significant change in the Au crystal structure (Figure 4) (Han et al. 2018). A notable performance of Au-based catalyst was reported by Xin et al. (2012) during glycerol oxidation. The catalyst enabled more profound glycerol oxidation, which favored complete oxidation to

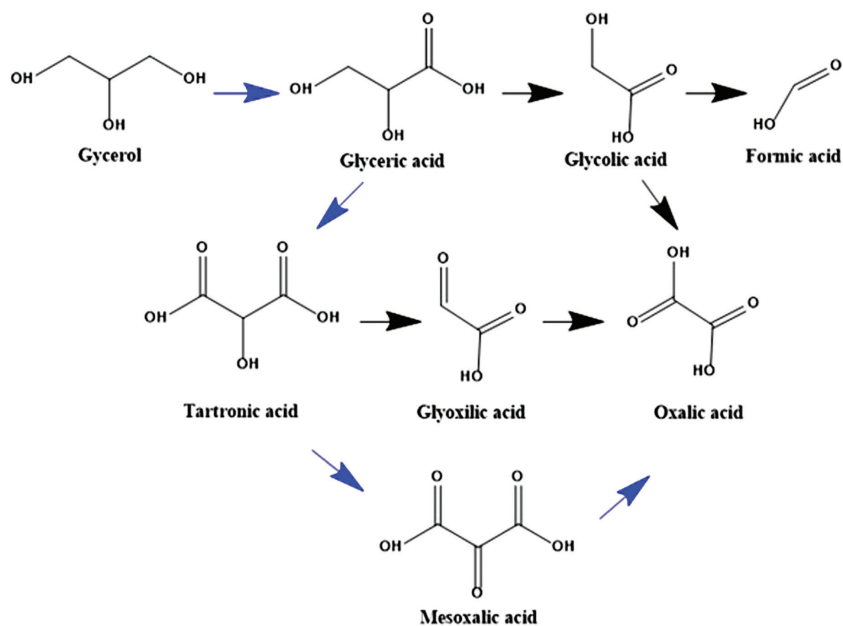


**Figure 3:** (A) CVs and (B) chronoamperometric curves for GEOR on Au-based and E-TEK Pt/C electrodes in 1.0 mol l<sup>-1</sup> KOH medium comprising 1.0 mol l<sup>-1</sup> glycerol at 298 K and -0.3 V (Zhang et al. 2016a).

Reproduced with kind permission from Elsevier (copyright license no. 4621230934217).



**Figure 4:** (A) XRD patterns of Au/C and ALD(TiO<sub>2</sub>)-Au/C. (B) TEM image of Au/C and (C) ALD(TiO<sub>2</sub>)-Au/C. Inset: Histograms of particle size distribution (Han et al. 2018). Reproduced with kind permission from Elsevier (copyright license no. 4621240229663).



**Scheme 4:** GEOR mechanism on some Au-based electrodes in a liquid-diffusion-electrode (LDE)–anion-exchange-membrane (AEM)-based electrolysis cell and fuel cell (green arrows represent the dominant pathways in a fuel cell) (Xin et al. 2012). Reproduced with kind permission from John Wiley and Sons (copyright license no. 4663451468002).

C3 mesoxalic acid, rather than C-C cleavage, under a small range of potentials (0.4–0.7 V vs. SHE). Fortunately, the potential is within the working voltage range of the fuel cells. Scheme 4 shows the reaction mechanism of glycerol

on the catalyst in a liquid-diffusion-electrode (LDE) anion-exchange-membrane (AEM)-based electrolysis cell and fuel cell. Table 4 presents the performance parameters of some Au-based electrodes during GEOR.

**Table 4:** Performance and product distribution of Au-based catalysts during GEOR.

Catalyst	GLY/Cat (mol:mol)	Anode potential (V)/membrane	Electrolyte formulation	Conv. (%)/ time (h)	Selectivity (%)					References	
					TA	GLA	DHA	GLAD	MOXA		GLCA
Au/C-NC	1:1300	<0.45 (vs. RHE)/AEMA901	8.0 M KOH+1.0 M glycerol, 30 ml, 60°C	54.9/4	70.67	15.12	-	-	2.13	2.13	Qi et al. (2014)
Au/C-NC	1:1300	<0.45 (vs. RHE)/AEMA901	8.0 M KOH+1.0 M glycerol, 30 ml, 60°C	77.4/8	69.64	14.47	-	-	1.74	2.13	Qi et al. (2014)
Au/C-NC	1:1300	<0.45 (vs. RHE)/AEMA901	8.0 M KOH+1.0 M glycerol, 30 ml, 60°C	89.3/12	69.06	14.11	-	-	0.75	2.13	Qi et al. (2014)
Au/C-AQ	1:1300	<0.45 (vs. RHE)/AEMA901	8.0 M KOH+1.0 M glycerol, 30 ml, 60°C	60.9/4	62.73	11.33	-	-	7.06	2.74	Qi et al. (2014)
Au/C-AQ	1:1300	<0.45 (vs. RHE)/AEMA901	8.0 M KOH+1.0 M glycerol, 30 ml, 60°C	84.4/8	62.68	11.75	-	-	4.68	2.42	Qi et al. (2014)
Au/C-AQ	1:1300	<0.45 (vs. RHE)/AEMA901	8.0 M KOH+1.0 M glycerol, 30 ml, 60°C	95.3/12	62.43	11.01	-	-	2.78	2.28	Qi et al. (2014)
Au/C	-	0.7 (vs. Hg/HgO)/-	0.1 M KOH+0.1 M glycerol, 60°C	10.7/0.5	4.9	50.3	-	-	-	13.7	Han et al. (2018)
ALD(TiO <sub>2</sub> )-Au/C	-	0.7 (vs. Hg/HgO)/-	0.1 M KOH+0.1 M glycerol, 60°C	11.9/0.5	4.8	64.9	-	-	-	21.6	Han et al. (2018)
Au/C	-	0.1 (vs. RHE)/AEMA201	2.0 M KOH+1.0 M glycerol, 80°C	37	37	26	-	-	12	3	Zhang et al. (2012c)
Au/C	-	0.3 (vs. RHE)/AEMA201	2.0 M KOH+1.0 M glycerol, 80°C	39	39	17	-	-	19	0	Zhang et al. (2012c)
Au/C	-	0.5 (vs. RHE)/AEMA201	2.0 M KOH+1.0 M glycerol, 80°C	49	49	26	-	-	0	0	Zhang et al. (2012c)

GLA, glyceric acid; TA, tartronic acid; DHA, dihydroxyacetone; GLAD, glyceraldehyde; GLCA, glycolic acid; MOXA, mesoxalic acid. Au/C-NC, Au/C catalysts prepared by the nanocapsule method; Au/C-AQ, Au/C catalysts prepared by aqueous-phase reduction method; Au-1/AC-THPC, prepared by gold-sol with tetrakis-(hydroxymethyl)-phosphonium chloride (THPC, 78 wt%); Au-1/AC-NaBH<sub>4</sub>, prepared by gold-sol with NaBH<sub>4</sub>; Au-1/AC-Prec, prepared by precipitation.

At high potential, Zhang et al. (2012e) proposed Scheme 5 using Au/CNT catalyst. Following this pathway, the selectivity of glycolate increases with increasing applied potential. About 85% selectivity of glycolate was achieved at 1.6 V, while 41% was achieved at 1.0 V. However, the selectivity of tartronate, oxalate, glycerate, and glycolate decreased with increasing applied potential.

### 3.4 Silver-based electrocatalysts

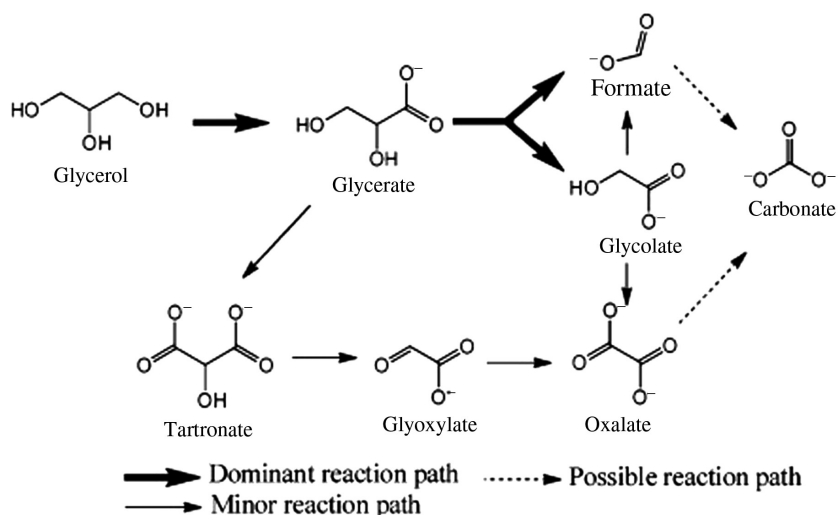
Monometallic catalysts such as Ag are suitable alternatives to noble metals like Au, Pd, and Pt for GEOR to produce value-added compounds. Compounds such as glycolic acid, glyceric acid, and formic acid have been produced using bulk Ag electrode electrooxidation of glycerol in an alkaline solution (Suzuki et al. 2016). Glycerol oxidation with Ag-based catalyst was reported for the first time in 1997 by Avramov-Ivić et al. (1997). They reported that Ag-based catalysts exhibit superior oxidation currents in a glycerol-containing electrolyte to those of ethylene glycol and methanol under similar conditions. The oxidation current declined with the increase in the scan rate, though no study on the charge of the process was performed. However, a recent study by Gomes et al. (2014b), using Ag nanoparticles as the electrocatalyst, found that the scan rate had no significant effect on the oxidation current during GEOR. Recently, Suzuki et al. (2016) studied the effect of glycerol concentration and electrolyte pH on GEOR kinetics. They found that increasing the concentration OH<sup>-</sup> boosted the oxidation current. A maximum of 2.3 mA cm<sup>-2</sup> current density in an electrolyte containing 1 M NaOH and 1 M glycerol gave the main products as formic acid, glyceric acid, and glycolic acid.

The product selectivity and distribution depend significantly on the amount of surface Ag rather than catalyst porosity and morphology (Thia et al. 2017). Thia et al. (2017) fabricated a series of Ag-containing porous Au structures by varying the operating parameters (etching time and subsequent annealing temperature) and applied them for the electrooxidation of glycerol. The dominant products observed were glycolate and formate for all the Ag-based samples despite the apparent difference in their morphology (Figure 5). Although Ag has been used as a co-catalyst with Au, Pd, and Pt, further studies are required to ascertain the suitability of Ag-based electrocatalysts for GEOR.

### 3.5 Nickel-based electrocatalysts

Nickel is a non-noble metal usually used as electrocatalyst in systems such as alcohol oxidation reactions in alkaline media (Zhang et al. 2013b, Oliveira et al. 2014, 2015), fuel





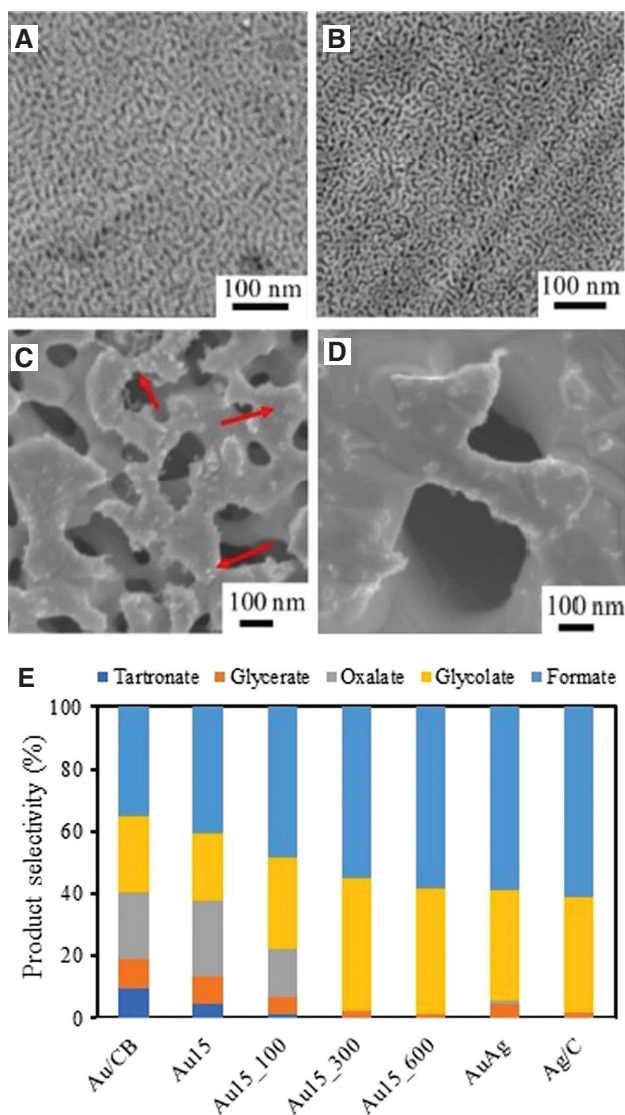
**Scheme 5:** Proposed reaction pathway for the electrooxidation of glycerol on Au/CNT catalyst at high potentials (Zhang et al. 2012e). Reproduced with kind permission from the Royal Society of Chemistry (copyright license no. 4663470224471).

cells (Faro et al. 2011), sensors (Tehrani and Ab Ghani 2012), alkaline batteries (Freitas 2001), and supercapacitors (Nam et al. 2002). The performance, efficiency, and catalytic activity of Ni are strongly influenced by the complexity of the Ni oxidation state surface chemistry in an alkaline electrolyte (Alsabet et al. 2015). However, several reports have shown that Ni exhibits remarkable electrocatalytic performance, durability in alkaline solutions, and anti-poison ability (Oliveira et al. 2013, 2014), making it a promising candidate for GEOR. Various Ni-based bimetallic Ni-M/C (M=Pt, Pd, Fe, Co) nanoparticles have also been employed as electrocatalysts (Caliman et al. 2013, Oliveira et al. 2013, 2014). Notably, the Pt<sub>2</sub>Ni/C catalyst exhibited a remarkable increase in reaction rate traceable to modification of its geometric and electronic structure when compared with the Pt/C catalyst. Pt<sub>2</sub>Ni/C shows superior catalytic performance in GEOR as revealed by a higher current density at a lower onset potential (Lee et al. 2012). Incorporation of Ni as a co-catalyst can considerably reduce the amount of Pt without penalizing the activity.

Specialty chemicals such as glycolate, glycerate, tartronate, formate, and oxalate have been produced successfully from Ni-based catalysts like Pd<sub>x</sub>Ni<sub>1-x</sub>/C, NiCoFe/C, NiCo/C, and Ni/C in alkaline media (Holade et al. 2013b, Oliveira et al. 2013, 2014). Holade et al. (2013b) proposed a pathway for glycerol oxidation on PdAg and PdNi in alkaline media (Scheme 5), which starts with the formation of glyceraldehyde and oxidation of the same to the glycerate ion. This is followed by the formation of three intermediates, namely glycolate, tartronate, and formate ions, depending on the applied potential and the nature of surface-active sites. The complexity of the reaction scheme suggests that it is critical

to have a good knowledge of the nature of the Ni surface active sites and their influence on product distribution in GEOR for the effective design of Ni-based electrocatalysts with enhanced performance. Scheme 6 shows a typical reaction mechanism for the selective oxidation of glycerol over a Ni-based electrocatalyst in an alkaline electrolyte.

Recently, Houache et al. (2018) investigated GEOR on treated and untreated Ni surfaces. The treatment was done by electrochemical sinusoidal-wave pretreatment in an ascorbic acid solution, following the study of Baranova et al. (2013). The pretreatment was tailored toward improving the suitability for the hydrogen evolution reaction (HER), which is promoted by surface Ni(OH)<sub>x</sub> (0 < x ≤ 2) formation. Morrison et al. (2016) and Houache et al. (2018) reported that before the treatment, the Ni surface comprises Ni metal as well as Ni(OH)<sub>2</sub>, NiOOH, and NiO. After pretreatment, the metallic surface decreased significantly; about 97% of the surface was Ni(OH)<sub>x</sub>, comprising Ni<sup>3+</sup> and Ni<sup>2+</sup>. The pretreatment helps to boost the current density for GEOR significantly (over 9 times), as observed from steady-state chronoamperometry (CA) experiments. Similar product selectivity was observed for both untreated and treated Ni surfaces since they exhibited comparable spectral features. The effect of modification of the Ni surface was illustrated by Han et al. (2017) in Figure 6, where Ni/C was modified by TiO<sub>2</sub> via the atomic layer deposition method. The deposition of Ti and O were observed to be even on the Ni/C surface, showing a significant alteration on the surface structure, although the crystalline face-centered cubic (fcc) phase of Ni was retained in both ALD(TiO<sub>2</sub>)-Ni/C and Ni/C (Figure 6C). Furthermore, modification with TiO<sub>2</sub> leads to enhanced formation of Ni(OH)<sub>2</sub> species, which are



**Figure 5:** FESEM images of the resulting Ag-based catalysts after 15 min etching and (A) no annealing, and successive annealing at (B) 100°C, (C) 300°C, and (D) 600°C. (E) Electrooxidation of glycerol in alkaline solution using the Ag-based catalysts (Thia et al. 2017). Reproduced with kind permission from the Royal Society of Chemistry.

active sites of the resulting ALD(TiO<sub>2</sub>)-Ni/C. The enhanced active sites make ALD(TiO<sub>2</sub>)-Ni/C exhibit superior electrocatalytic performance and durability in comparison to Ni/C for glycerol electrooxidation.

### 3.6 Multimetallic catalysts

#### 3.6.1 Bimetallic

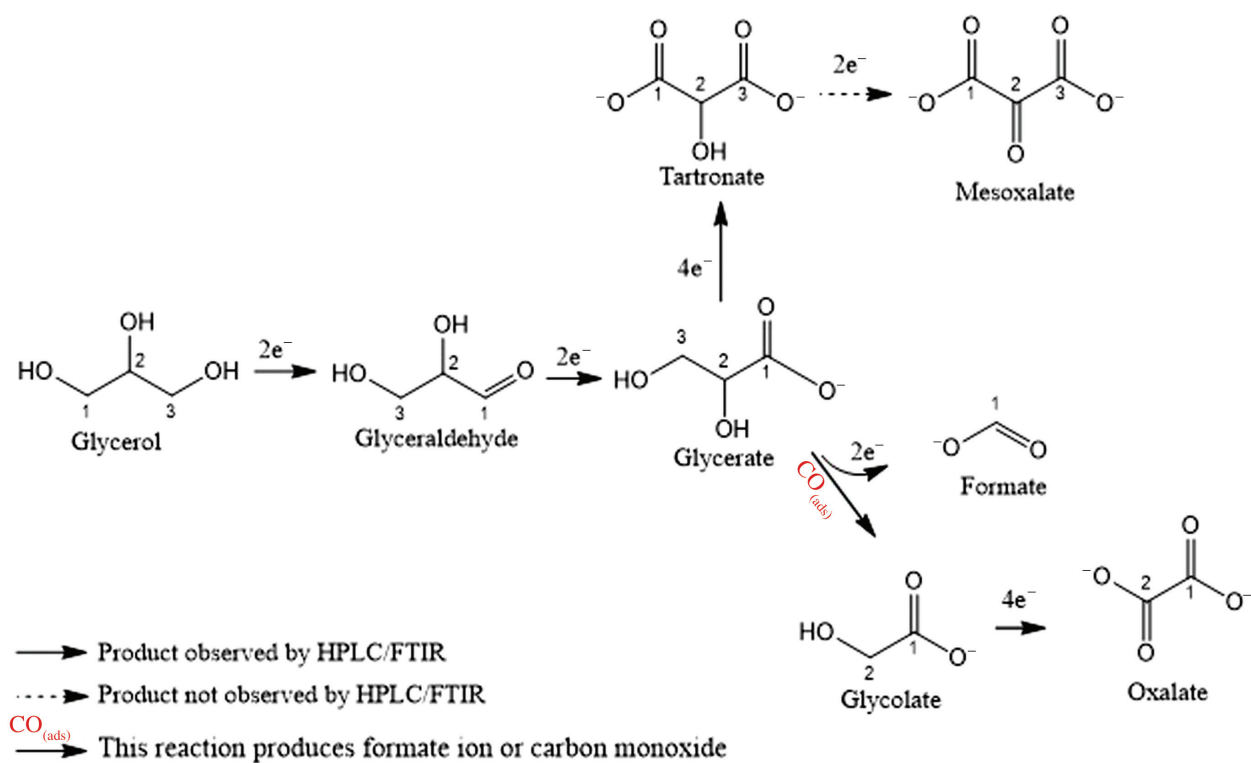
Although Pt-, Pd-, and Au-based materials are popular anode catalysts for the electrooxidation of small organic

molecules, using them as monometals is faced with various drawbacks (Table 5). These drawbacks necessitate the consideration for the alloying of these metals by rationally designing a single material from two or three of them (Benipal et al. 2018). The alloying could help enhance the electronic structure of the catalyst and suppress the poisoning of active sites induced by carbonaceous compounds (Rostami et al. 2017). Bimetallic catalysts possess a unique microstructure (as revealed in Figure 7), exhibiting higher forward peak current densities and better facilitation of C-C bond cleavage due to the synergistic effects of their constituents, relative to their monometal counterparts (Zhou and Shen 2018).

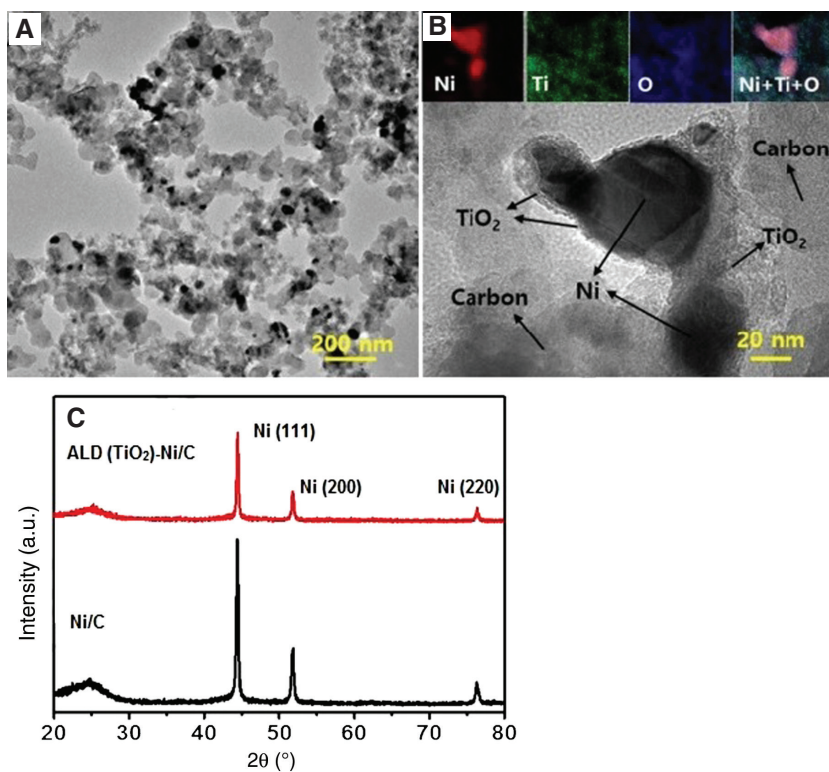
Several authors have reported the remarkable activity of bimetallic electrocatalysts for GEOR. Kim et al. (2014) found that PtAg nanotubes exhibit enhanced performance as anode catalysts for GEOR when compared with conventional Pt/C and Pt nanotubes. The enhanced performance was evident in poisoning suppression, lower onset potential, and the peak current density. The synergistic incorporation of different metallic species creates a better microstructure which facilitates the cleavage of the C-C bond, thereby improving the oxidation of CO and other carbonaceous compounds in the reactor (Kim et al. 2011a). Modifying Pt/C with Bi could minimize the oxidation onset potential relative to that of Pt/C catalyst. Also, substituting half of the Pt atoms with Pd atoms could achieve catalytic activity similar to that with PtBi/C without altering the reaction pathway (Scheme 7) (Simões et al. 2011). Silva et al. (2016) developed a core-shell hybrid Pt and Pb carbide (Pb<sub>x</sub>@Pt<sub>y</sub>/C) by successive reduction methods without the help of surfactants. The combined surface structure exhibited a unique electronic effect and durability, which demonstrated remarkable activity during GEOR.

Pt has also been used as a co-catalyst with rhodium (Rh) because Rh, being oxophilic, promotes the cleavage of the C-C bond and produces OH<sub>ads</sub> at a lower anode potential, thereby facilitating oxidative desorption of carbonaceous intermediate species (Erini et al. 2014, Zanata et al. 2016). Zanata et al. (2016) studied the electrocatalytic activity and stability of Rh-decorated PtIrO<sub>x</sub>/C during GEOR. While the presence of Rh promotes C-C cleavage, Ir helps to intensify the electronic effect and prevent agglomeration, thereby improving the activity and stability. The reports of Wesselmark et al. (2013) and Reier et al. (2012) also corroborate the impact of Ir as a stability promoter.

Furthermore, oxides such as NiO<sub>x</sub> and MnO<sub>x</sub> could intensify the electronic effect of noble metal-based electrocatalysts because of their potential in regulating the electron extraction/injection properties of the electrodes



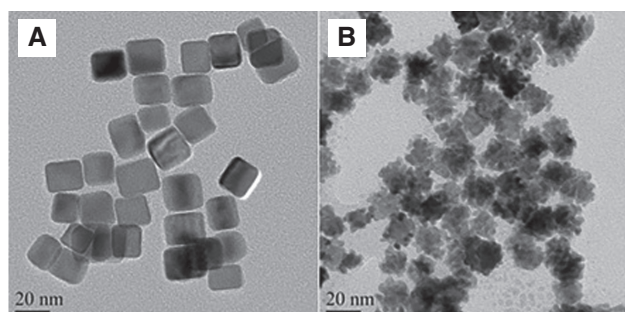
**Scheme 6:** Proposed reaction pathway for GEOR on Ni-based nanocatalyst in alkaline solution. The dotted arrows denote that the product was not clearly obtained by HPLC (Holade et al. 2013b). Reproduced with kind permission from the American Chemical Society.



**Figure 6:** (A) TEM and (B) HRTEM images of ALD(TiO<sub>2</sub>)-Ni/C. (D) XRD patterns of Ni/C and ALD(TiO<sub>2</sub>)-Ni/C (Han et al. 2017). Reproduced with kind permission from Elsevier (copyright license no. 4621230294510).

**Table 5:** Merits and demerits of some monometal-based electrocatalysts.

Catalyst	Merit	Demerit	References
Pt-based	Active under basic and acidic conditions	Expensive. Slower in acidic solutions than in basic solutions due to the slow kinetics. Prone to poisoning by carbonaceous intermediate species	Dodekatos et al. (2018), Xu and Zhang (2014)
Pd-based	Active under basic acidic conditions. Less expensive, more abundant, and better tolerant to poisoning than Pt	Need to improve the poison tolerance and durability	Dodekatos et al. (2018), Hu and Wang (2015), Zalineeva et al. (2015a), Zhang and Shen (2013)
Au-based	Enhanced resistances to oxygen and poisoning carbonaceous intermediate species. Less expensive compared to Pt and Pd. Promotes C-C cleavage to produce C2 and C1 compounds	Only active under basic aqueous conditions	Dodekatos et al. (2018), Zhang et al. (2016a)
Ag-based	Less expensive when compared to Pt and Pd. Promotes C-C cleavage to produce C2 and C1 compounds. Suitable promoter for Pt, Pd, and Au	Weak performance. Oxidation reaction is blocked at potentials $>1.125$ V, irrespective of glycerol concentration in the solution	Suzuki et al. (2016), Thia et al. (2017)
Ni-based	Remarkable catalytic activity comparable to Pt, Pd, and Au. Cheap, durable in alkaline solutions and able to resist poisoning	Only active under basic aqueous conditions	Ashok et al. (2019), Hajar et al. (2017)

**Figure 7:** TEM images of (A) Pd NCs and (B) Pt@Pd NPs (Zhou and Shen 2018).

Reproduced with kind permission from Elsevier (copyright license no. 4621260644141).

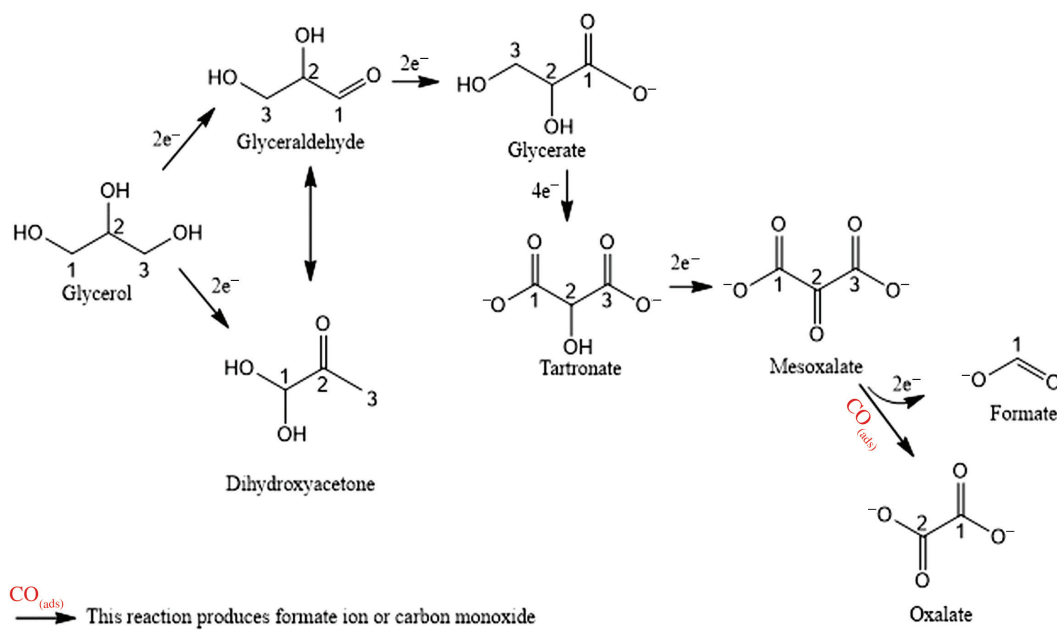
(Greiner et al. 2012). The incorporation of these oxides helps in lowering the affinity of noble metals such as Pt to generate surface  $\text{PtO}_x$  species, making the carbonaceous intermediate species formed to be less strongly adsorbed on Pt. The oxides can be a source of oxygenated species needed for GEOR to ensure optimal catalytic surface (Garcia et al. 2017).

Furthermore, bimetallic catalysts such as PdNi, PdPb, or PdAg nanoparticles are suitable catalysts for the electrooxidation of alcohols (Singh and Singh 2009, Simões et al. 2010, Xu et al. 2018). While Pd only facilitates alcohol deprotonation in alkaline media with low C-C cleavage ability, the incorporation of Ag to Pd promotes glycerol oxidation by facilitating C-C bond cleavage of  $\text{C}_3$  species to  $\text{C}_2$  and oxidation of the intermediate species (Wang et al.

2010, Ferreira et al. 2013, Benipal et al. 2017). When Ag is added to Pd, the d-band center is altered by the larger lattice parameter of Ag ( $a=4.09$  Å) (Holade et al. 2013a). Incorporation of Ni offers a similar beneficial effect to Pd during the ethanol oxidation reaction (Shen et al. 2010). This is because Ni species are oxophilic like Rh, which can generate  $\text{OH}_{\text{ads}}$  at a lesser potential, thereby facilitating the oxidative removal of carbonaceous intermediate species to improve both the stability and activity of Pd catalysts (Holade et al. 2013a). Holade et al. (2013a) confirmed the activity and stability of PdAg/C and PdNi/C nanocatalysts during GEOR. They found both catalysts exhibiting superior kinetics in comparison with Pd/C. PdAg has also been successfully supported on CNTs, and proven to be more effective than Pd during glycerol oxidation (Qi et al. 2016, Benipal et al. 2017). The presence of Ag favors C-C bond cleavage and more profound oxidation, thus promoting the selectivity of  $\text{C}_2$  species such as glycolate and oxalate.

Alloying Au with Pd can enhance the catalytic activity of a Pd-based catalyst during GEOR by improving  $\text{OH}^-$  adsorption on the catalyst surface in an alkaline electrolyte, which reduces the onset potential (Mougenot et al. 2011). The electronic interactions of Au with Pd could minimize the binding energy of adsorbed carbonaceous intermediate products on the active sites of Pd, thereby suppressing poisoning and boosting the catalytic activity (Xu et al. 2017). Xu et al. (2017) developed an N-doped, graphene-supported PdAu alloy (PdAu-NF/NG) using a facile ultrasonic-assisted technique. Their report revealed that the as-prepared catalyst exhibited an unusual mass





**Scheme 7:** Reaction mechanism proposed for the electrooxidation of glycerol on  $\text{Pd}_{0.9}\text{Bi}_{0.1}/\text{C}$ ,  $\text{Pt}_{0.9}\text{Bi}_{0.1}/\text{C}$ , and  $\text{Pd}_{0.45}\text{Pt}_{0.45}\text{Bi}_{0.1}/\text{C}$  catalysts (Simões et al. 2011).

Reproduced with kind permission from Elsevier (copyright license no. 4663480509132).

activity of  $8.7 \text{ A mg}^{-1}$  for glycerol oxidation. This is about 12.25 times greater than that of the conventional  $\text{Pd}/\text{C}$  catalyst ( $0.71 \text{ A mg}^{-1}$ ).

For industries that require formic acid as a raw material in processes like food additives, grass silage, textile dyeing and finishing, anti-icing, leather tanning, drilling fluids, and natural rubber, AuAg alloy is promising (Thia et al. 2017). Typically, the use of a Ag (polycrystalline) monometallic catalyst for GEOR in alkaline media favors the formation of formate, glycerate, and glycolate, but at high potentials [above 1.13 V(vs. RHE)], adsorption of  $\text{OH}^-$  and glycerol becomes impossible due to the formation of surface  $\text{Ag}_2\text{O}$  (Garcia et al. 2014, Gomes et al. 2014a). It is important to note that Au/C is highly active for glycerol electrooxidation, while Ag/C is a very poor catalyst for the reaction (Gomes et al. 2014a).

The rational design of a suitable catalyst demands that the catalyst possesses Au-rich surfaces. This will enable high selectivity toward formic acid without jeopardizing the electrochemical activity (Garcia et al. 2014). Garcia et al. (2014) fabricated Ag-based catalysts covered with Au surfaces for glycerol oxidation. The produced catalysts exhibited a porous Au-rich structure with residual Ag inside its pores. They reported that the as-prepared catalyst displayed both remarkable catalytic activity and high selectivity towards formate. Table 6 presents the performance parameters of some different bimetallic electrodes during GEOR.

### 3.6.2 Trimetallic catalysts

A trimetallic catalyst with a rationally designed composition and framework can offer new perceptions on the catalytic activity, selectivity, and durability of noble metal-based materials, which are not often reported relative to noble metal-based mono and bimetallic materials. The reports of Rostami et al. (2017) and Zhou et al. (2018) revealed that rationally designed trimetallic catalysts (by optimizing the composition) could exhibit superior performance to bimetallic and monometallic catalysts. Because of the synergistic effect of the constituents, well-designed ternary catalysts possess low onset potentials and high current densities, thereby facilitating complete oxidation of poisonous carbonaceous species (Kim et al. 2011a). Techniques such as sol-gel, seed-mediated growth, galvanic replacement, and thermal decomposition have been studied toward developing Pt-based trimetallic NCs in pioneering researches (Liu et al. 2014, Huan et al. 2015). For instance, Rezaei et al. (2016) rationally fabricated a Cu-deposited nanoporous stainless steel catalyst covered with Pt and Pd ( $\text{Pt-Pd}/\text{Cu}/\text{NPSS}$ ) for the electrooxidation of glycerol in alkaline media. Cyclic voltammetry studies revealed that at the lower onset potential of  $-0.54 \text{ V}$ ,  $\text{Pt-Pd}/\text{Cu}/\text{NPSS}$  displayed higher resistance to poisoning by carbonaceous intermediate species and higher current density by a factor of 4.2 when compared with  $\text{Pd}/\text{Cu}/\text{NPSS}$ ,  $\text{Pt}/\text{Cu}/\text{NPSS}$ , and pure Pt catalysts.



**Table 6:** Performance of the different bimetallic catalysts for glycerol electrooxidation.

Catalyst	Electrolyte (M KOH + M GLY)	$E_{\text{onset}}$ (V vs. RHE)	$I_p$ (A mg <sup>-1</sup> )	EASA (cm <sup>2</sup> mg <sup>-1</sup> )	References
PtAg/C	1.0+1.0	0.176	2.25		Garcia et al. (2014)
PtAg/MnO <sub>x</sub> /C	1.0+1.0	0.184	3.04		Garcia et al. (2014)
Rh/Pt <sub>95</sub> (IrO <sub>x</sub> )/C	0.1 (HClO <sub>4</sub> )+0.2	0.47	0.0077	–	Zanata et al. (2016)
Pbx@Pty/C core-shell	0.5 (H <sub>2</sub> SO <sub>4</sub> )+0.5	0.52	4.36 mA cm <sup>-2</sup>	1600	Silva et al. (2016)
Pb@Pt <sub>2</sub> /C	0.5 (H <sub>2</sub> SO <sub>4</sub> )+0.5	0.43	3.76 mA cm <sup>-2</sup>	1440	Silva et al. (2016)
Pb <sub>2</sub> @Pt/C	0.5 (H <sub>2</sub> SO <sub>4</sub> )+0.5	0.52	2.62 mA cm <sup>-2</sup>	1832	Silva et al. (2016)
Pb@Pt <sub>3</sub> /C	0.5 (H <sub>2</sub> SO <sub>4</sub> )+0.5	<0.36	5.08 mA cm <sup>-2</sup>	2673	Silva et al. (2016)
Pd <sub>60</sub> Ag <sub>40</sub> /C	0.1 (NaOH)+0.1	0.5	0.252	310	Holade et al. (2013a)
Pd <sub>60</sub> Ni <sub>40</sub> /C	0.1 (NaOH)+0.1	0.5	0.148	–	Holade et al. (2013a)
Pd <sub>3</sub> Ru-PEDOT/C	1.0 NaOH+0.1	–0.438 (vs. SCE)	4.3 mA cm <sup>-2</sup>	–	Dash and Munichandriah (2015)
FeCo@Fe@Pd/MWCNT-COOH	1.0+0.5	–0.57 (vs. Ag/AgCl)	17.8 mA cm <sup>-2</sup>	746.3	Fashedemi et al. (2015)
PdAg/CNT	1.0+0.1	–0.39 (vs. MMO)	43.9 mA cm <sup>-2</sup>	–	Benipal et al. (2017)
PdAg <sub>3</sub> /CNT	1.0+0.1	–0.44 (vs. MMO)	35.4 mA cm <sup>-2</sup>	–	Benipal et al. (2017)
Pd/Cu/NPSS	1.0+5 wt%	–0.35	23.8 mA cm <sup>-2</sup>	173.4	Rezaei et al. (2016)
Pd-Au/NPSS	1.0+5 wt%	–0.33(vs. SHE)	134 mA cm <sup>-2</sup>	62.5	Rezaei et al. (2016)
Co-sputtered Pd <sub>0.7</sub> Au <sub>0.3</sub>	1.0 (NaOH)+0.1	0.1	25.8 mA cm <sup>-2</sup>	226	Mougenot et al. (2011)
PdAu-NF/NG	1.0+1.0	–/SCE	8.7	1365.2	Xu et al. (2017)
Ag/Pd	1.0+0.5	–0.25 (vs. Hg/HgO)	52.1 mA cm <sup>-2</sup>	–	Inoue et al. (2018)
PdAg/CNT	1.0+0.1	0.5	8.53	–	Qi et al. (2016)
PdAg <sub>3</sub> /CNT	1.0+0.1	0.5	6.91	–	Qi et al. (2016)
Pd <sub>50</sub> Ag <sub>50</sub> /C	0.1 (NaOH)+0.1	0.50	0.263	–	Holade et al. (2013a)
Pd <sub>50</sub> Ni <sub>50</sub> /C	0.1 (NaOH)+0.1	0.45	0.190	–	Holade et al. (2013a)
PdRh	0.1+0.1	–	1.16 mA cm <sup>-2</sup>	–	Holade et al. (2013a)
Pd <sub>55</sub> Pt <sub>30</sub> NNWs	1.0+0.1	–	0.046 A cm <sup>-2</sup>	222	Brouzgou et al. (2014)
Pt <sub>0.9</sub> Bi <sub>0.1</sub> /C	1.0 (NaOH)+0.1	0.2	31.6 mA cm <sup>-2</sup>	–	Simões et al. (2011)
Pd <sub>0.45</sub> Pt <sub>0.45</sub> Bi <sub>0.1</sub> /C	1.0 (NaOH)+0.1	0.2	38.5 mA cm <sup>-2</sup>	–	Simões et al. (2011)
Pd <sub>90</sub> Ag <sub>10</sub> /C	0.1 (NaOH)+0.1	0.54	0.138	470	Holade et al. (2013a)
Pd <sub>80</sub> Ag <sub>20</sub> /C	0.1 (NaOH)+0.1	0.54	0.136	160	Holade et al. (2013a)
Pd <sub>70</sub> Ag <sub>30</sub> /C	0.1 (NaOH)+0.1	0.56	0.185	340	Holade et al. (2013a)
Pd <sub>60</sub> Ag <sub>40</sub> /C	0.1 (NaOH)+0.1	0.5	0.253	720	Holade et al. (2013a)
Pd <sub>50</sub> Ag <sub>50</sub> /C	0.1 (NaOH)+0.1	0.5	0.263	720	Holade et al. (2013a)
Pd <sub>90</sub> Ni <sub>10</sub> /C	0.1 (NaOH)+0.1	0.52	0.149	–	Holade et al. (2013a)
Pd <sub>80</sub> Ni <sub>20</sub> /C	0.1 (NaOH)+0.1	0.52	0.177	–	Holade et al. (2013a)
Pd <sub>70</sub> Ni <sub>30</sub> /C	0.1 (NaOH)+0.1	0.52	0.175	–	Holade et al. (2013a)
Pd <sub>60</sub> Ni <sub>40</sub> /C	0.1 (NaOH)+0.1	0.45	0.148	–	Holade et al. (2013a)
Pd <sub>50</sub> Ni <sub>50</sub> /C	0.1 (NaOH)+0.1	0.46	0.19	–	Holade et al. (2013a)

Rostami et al. (2015) developed a trimetallic electrocatalyst by the electrodeposition of a Pd-Co alloy on Au surface for GEOR in an alkaline medium. The as-prepared Pd-Co(III)/Au exhibited remarkably superior current density at a lesser onset potential and better tolerance to poisoning when compared with Pd/Au. The presence of Co promoted the tolerance to poisoning. Fashedemi et al. (2015) fabricated a Pd-based ternary core-shell (FeCo@Fe@Pd) nanocatalyst supported by MWCNTs functionalized with carboxylic and sulfonic acids via microwave-induced top-down nanostructuring and decoration. The synergistic effect of the metals culminated in remarkable catalytic performance in the electrocatalytic oxidation of glycerol. The catalytic performance was further improved

by functionalization, which had a noteworthy impact on the physicochemical properties of the FeCo@Fe@Pd nanocatalyst.

Moreover, modification of the electrocatalysts with Au substrate has been found to result in superior catalytic activity when compared with a carbon substrate (Venancio et al. 2002). This reveals that Pt and Au exhibit a remarkable synergistic effect. In a recent study, Zhou et al. (2019) confirmed the beneficial impact of a Au substrate on Pt-based trimetallic catalysts using Ag nanoparticles as sacrificial seeds. The as-prepared Pt<sub>x</sub>Au<sub>y</sub>@Ag nanoparticles exhibited better catalytic activity than the Pt/C catalyst during GEOR in both acidic and alkali media. The current density of Pt<sub>x</sub>Au<sub>y</sub>@Ag could be up to 2.6 times higher than

**Table 7:** Performance of the different trimetallic catalysts for glycerol electrooxidation.

Catalyst	Electrolyte (M KOH + M GLY)	$E_{\text{onset}}$ (V vs. RHE)	$I_p$ (A mg <sup>-1</sup> )	EASA (cm <sup>2</sup> mg <sup>-1</sup> )	References
Pt-Pd/Cu/NPSS	1.0 + 5.0 wt%	-0.54 V	59.96	223.5	Rezaei et al. (2016)
Pd-Co(1)/Au	1.0 + 1.0	-0.37	115.2 mA cm <sup>-2</sup>		Rostami et al. (2015)
Pd-Co(2)/Au	1.0 + 1.0	-0.43	133.1 mA cm <sup>-2</sup>		Rostami et al. (2015)
Pd-Co(3)/Au	1.0 + 1.0	-0.43	183.3 mA cm <sup>-2</sup>		Rostami et al. (2015)
Pd-Co(4)/Au	1.0 + 1.0	-0.41	102.7 mA cm <sup>-2</sup>		Rostami et al. (2015)
Pt <sub>2</sub> Au <sub>8</sub> @Ag	1.0 (HClO <sub>4</sub> ) + 1.0		0.0252 mA cm <sup>-2</sup>		Zhou et al. (2019)
Pt <sub>3</sub> Au <sub>7</sub> @Ag	1.0 (HClO <sub>4</sub> ) + 1.0	0.59	0.0368 mA cm <sup>-2</sup>		Zhou et al. (2019)
Pt <sub>4</sub> Au <sub>6</sub> @Ag	1.0 (HClO <sub>4</sub> ) + 1.0	0.437	0.154 mA cm <sup>-2</sup>		Zhou et al. (2019)
Pt <sub>5</sub> Au <sub>5</sub> @Ag	1.0 (HClO <sub>4</sub> ) + 1.0	0.39	0.267 mA cm <sup>-2</sup>		Zhou et al. (2019)
Pt <sub>6</sub> Au <sub>4</sub> @Ag	1.0 (HClO <sub>4</sub> ) + 1.0	0.393	0.251 mA cm <sup>-2</sup>		Zhou et al. (2019)
Pt <sub>7</sub> Au <sub>3</sub> @Ag	1.0 (HClO <sub>4</sub> ) + 1.0	0.37	0.267 mA cm <sup>-2</sup>		Zhou et al. (2019)
Pt <sub>2</sub> Au <sub>8</sub> @Ag	0.1 + 1.0	0.481	1.48		Zhou et al. (2019)
Pt <sub>3</sub> Au <sub>7</sub> @Ag	0.1 + 1.0	0.481	2.34		Zhou et al. (2019)
Pt <sub>4</sub> Au <sub>6</sub> @Ag	0.1 + 1.0	0.488	2.50		Zhou et al. (2019)
Pt <sub>5</sub> Au <sub>5</sub> @Ag	0.1 + 1.0	0.481	1.55		Zhou et al. (2019)
Pt <sub>6</sub> Au <sub>4</sub> @Ag	0.1 + 1.0	0.567	1.50		Zhou et al. (2019)
Pt <sub>7</sub> Au <sub>3</sub> @Ag	0.1 + 1.0	0.531	0.672		Zhou et al. (2019)

that of Pt/C in acidic media and 4.7 times higher in alkaline media. Furthermore, Pt<sub>x</sub>Au<sub>y</sub>@Ag exhibited excellent selectivity toward C<sub>3</sub> compounds due to the synergistic impact of Au/Ag and Pt atoms as well as the dominant Pt(111) surfaces in Pt<sub>x</sub>Au<sub>y</sub>@Ag. Table 7 presents the performance parameters of some trimetallic electrodes during GEOR.

## 4 Untapped possible catalyst formulations

### 4.1 Heteroatom-doped metal-free electrocatalysts

Heteroatom-doped metal-free materials have become prominent electrocatalysts in fuel cell systems. In the past decades, N-doped carbon-based electrocatalysts have been successfully used for oxygen reduction reaction (ORR), yielding promising material design (Bayatsarmadi et al. 2015, Liu et al. 2016). Heteroatom doping on carbon material induces variation in spin densities and electronic charge densities in a carbon matrix, which disturbs the electroneutrality, thereby creating many catalytically active sites suitable for ORR (Yang et al. 2015, Hoyt et al. 2016). Literature shows that the same catalyst used for ORR can also be used for the oxygen evolution reaction (OER) (Yue et al. 2017, Mamtani et al. 2018). Several authors have reported N-doped carbon nanostructures

(CN<sub>x</sub>) as a promising bifunctionality for OER and ORR similar to the conventional Pt/C-fabricated N-doped CNTs (CNNTs) with varying pore size distribution (Zhao et al. 2013, Mamtani and Ozkan 2015, Yadav et al. 2015, Song et al. 2016). They reported that CNNT is a viable bifunctional electrocatalyst for both ORR and OER. Increase in the CNNT pore diameter improves the catalytic activity by enhancing the conductivity and reducing the oxygen adsorption energy, thereby facilitating the reactions by boosting the N-induced active sites in CNNT. Zhao et al. (2013) found that N-doped carbon material exhibits 10 mA cm<sup>-2</sup> current density at 0.38 V overpotential and is efficient for OER.

Several researchers have studied boron (B)-doped carbon, and reported the synergetic effect exhibited by B and N co-doped carbon for ORR due to the contrary electronic properties of B and N. Using both theoretical and experimental approaches, scholars have studied metal-free materials such as carbon doped with a halogen like fluorine (F), iodine (I), bromine (Br), or chlorine (Cl) (Yang et al. 2011b, Yao et al. 2012, Sun et al. 2013a), sulfur (S), silicon (Si), phosphorus (P) (Yang et al. 2011b, Yao et al. 2012, Yu et al. 2012), and their mixtures (Liang et al. 2012, Yu et al. 2012, Zhang et al. 2014). According to quantum chemical computations, the variance in electronegativity between the heteroatom dopants (S=2.58, N=3.04, P=2.19, B=2.04, I=2.66, Br=2.96, and Cl=3.16) and C atom (2.55) (Sun et al. 2013b) in the framework of covalently doped graphitic carbon is capable of polarizing adjacent C atoms to generate net negatively/positively charged centers that can enable electron transfer (Gong

et al. 2009). For instance, it is on record that C doping with F or both N and F can alter its electronic structure to generate highly efficient active sites for ORR (Liang et al. 2012). Furthermore, first-principles computations revealed that Si-doping could tune the electronic structure of carbon materials to enhance their catalytic activity (Zhang and Dai 2012).

Gong et al. (2009) found that the catalytic activity and durability of vertically aligned N-doped CNT arrays (VA-NCNTs) in an alkaline electrolyte exceeded those of the conventional Pt/C for ORR. Based on first-principles computations, N with high electron affinity in the framework of carbon materials can stimulate a positive charge density on adjacent C atoms, thereby weakening the O-O bond and facilitating oxygen adsorption (Chen et al. 2009). Despite the smaller electronegativity of B compared to N, several researchers have used it to dope quite a number of carbon materials such as diamond, graphene sheets, and CNT, and the resulting catalysts have proven efficient for ORR (Yang et al. 2011a, Sheng et al. 2012, He et al. 2014).

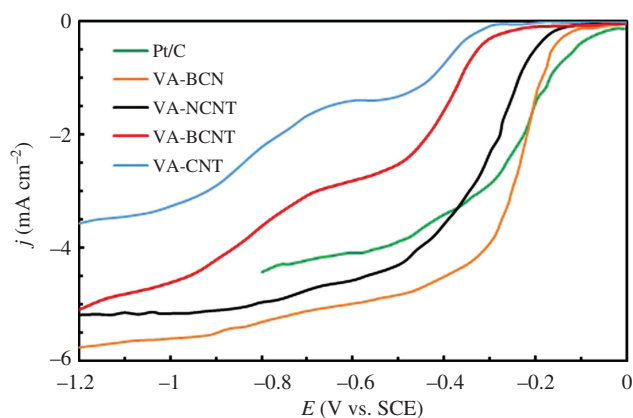
S-doped carbon material is also reported as a suitable electrocatalyst for ORR based on catalytic activity and stability, but it is not as good as N-doped material. Chen et al. (2014), Yang et al. (2011c, 2012) demonstrated this using S-doped graphene for ORR in alkaline media. S-doping helps to boost the spin density of graphene and influence the electron transfer. Similar to S and B, P-doped carbon materials like mesoporous carbon (Yang et al. 2012), nanospheres (Liu et al. 2012), nanotubes (Liu et al. 2011), and graphene (Zhang et al. 2013a) have been reported for ORR. Some theoretical computations revealed that P-doping on graphene influences its bandgap, with a more noticeable result than obtained with S-doping (Denis 2010, 2013). Incorporation of P on carbon materials improves their electron transfer properties, thereby enhancing the catalytic activity for ORR (Strelko et al. 2000).

Recently, Yao et al. (2012) investigated halogen-doped carbon materials as catalysts for ORR. I-doped graphene was rationally prepared by a facile thermal annealing technique. Doping with  $I_3^-$  favored a higher positive charge density on the surface of graphene, thereby promoting the reaction by reducing oxygen to  $OH^-$ . Rationally designed I-doped carbon species could offer a higher catalytic activity than conventional Pt/C during ORR (Yao et al. 2012). Jeon et al. (2013) comparatively studied three different halogen (I, Br, and Cl)-doped graphene nanoplates during ORR. They reported that halogen-doped graphene nanoplates are promising electrocatalysts for ORR.  $I_2$ -doped substrate exhibited the highest catalytic activity, while the  $Cl_2$ -doped one exhibited the least, which is contrary to the doping-influenced charge transfer mechanism since the

halogen electronegativities follow  $I (2.66) < Br (2.96) < Cl (3.16)$  (Liu et al. 2015). The superior performance of I and Br could be due to them possessing a larger atomic size than Cl, making the valence electrons of I and Br less tightly bound and simpler to loosen than those of Cl, thereby enabling charge polarization in the I-doped and Br-doped electrodes (Jeon et al. 2013).

Co-doping multiple heteroatoms with higher electronegativity difference induces defects that engender high spin densities and maximum charge redistribution, thereby producing many active sites that synergistically facilitate ORR activity (Li et al. 2017, Liu et al. 2018a, Zhan et al. 2018). Since there is a reverse electronegativity between N and B when compared with carbon, which could effectively detract the electroneutrality in the carbon matrix (Zhang et al. 2016b, 2017a,b), incorporating N and B into the C matrix can synergistically tune the electronic structure to favor ORR (Zhang et al. 2014). Co-doping of a heteroatom was first demonstrated by Ernst et al. (2011) and Ozaki (2006) and subsequently by Wang et al. (2011) and Zhang et al. (2014). For instance, vertically aligned CNTs (VACNTs) co-doped with N and B (VA-BCN) (Wang et al. 2011, Zhang et al. 2014) demonstrated the synergetic impacts of N- and B co-doping (VA-BCN), which exhibited superior ORR performance than the single-doped VA-BCNT and VA-NCNT, as well as Pt/C (Figure 8).

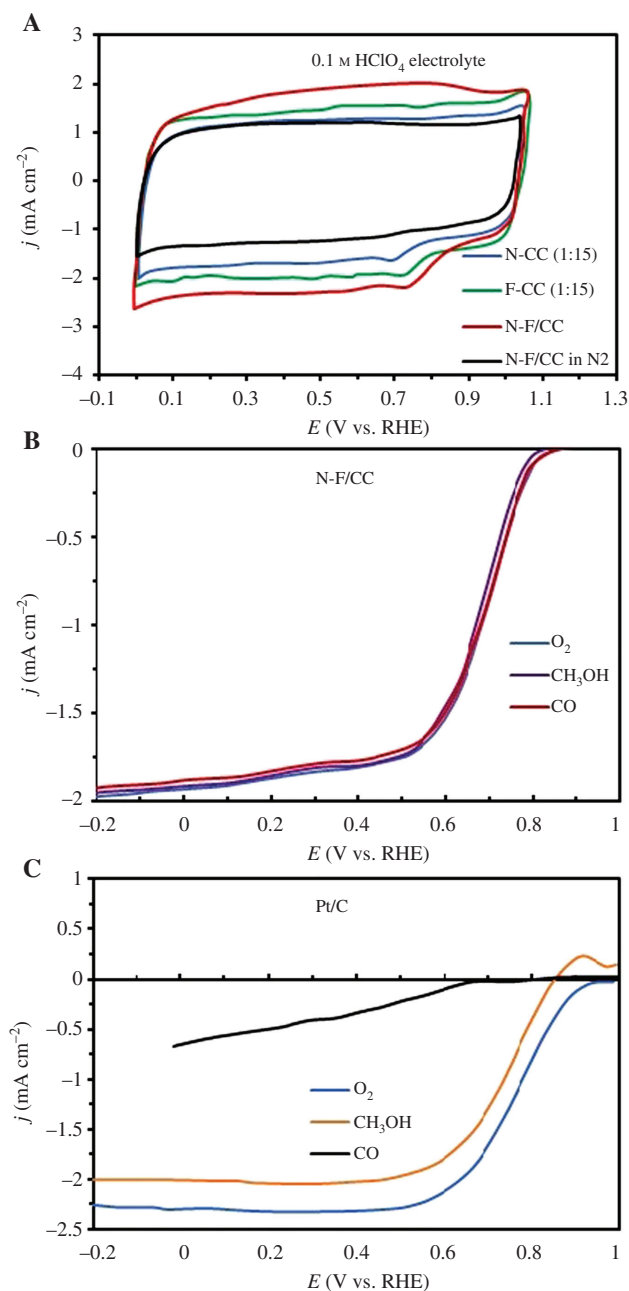
Several studies have reported the suitability of N and F co-doped mesoporous carbon, showing that the performance of the metal-free electrocatalyst is similar to that of the conventional Pt/C, with  $CH_3OH$  and CO tolerance and stability in alkaline solutions. Akula and Sahu (2019) fabricated mesoporous carbon simultaneously doped with N



**Figure 8:** LSV curves of some electrodes in oxygen-saturated 0.1 M KOH solution at a scan rate of  $10 \text{ mV s}^{-1}$  and 1000 rpm rotation (Wang et al. 2011).

Reproduced with kind permission from John Wiley and Sons (copyright license no. 4621420039670).

and F (N-F/CC). They reported that N-F/CC exhibited the best  $E_{\text{Red}}$  potential (0.73 V) when compared to individually doped CC, demonstrating a synergistic effect between the dopants (Figure 6A). Moreover, N-F/CC exhibited higher ORR performance than conventional Pt/C in 0.1 M  $\text{HClO}_4$



**Figure 9:** (A) Cyclic voltammograms (CVs) of CC, N-CC, F-CC, and N-F/CC catalysts at  $50 \text{ mV s}^{-1}$ . (B) LSVs for N-F/CC catalyst in presence of  $\text{O}_2$ ,  $\text{CO}$ ,  $\text{CH}_3\text{OH}$  species recorded at 1600 rpm in aqueous 0.1 M KOH at the scan rate of  $5 \text{ mV s}^{-1}$ , respectively. (C) The corresponding sensitivity tests for Pt/C (Akula and Sahu 2019). Reproduced with kind permission from Electrochemical Society (copyright license no. 4621410045209).

solution (Figure 6B), taking advantage of the synergistic effect exerted by simultaneous co-doping F and N on the carbon matrix. The catalyst showed superior electrochemical stability, great activity and CO vulnerability in alkaline and acidic media, and cost effectiveness. The superior stability of the co-doped material is because N doping in the presence of F improves charge delocalization and spin-density enhancement via attack from the basal plane of the carbon matrix (Gao et al. 2015, Peera et al. 2015, Akula et al. 2017). Furthermore, the catalytic activity of N-F/CC during ORR is not affected by the addition of  $\text{CO}$  or  $\text{CH}_3\text{OH}$  in alkaline media, as in the case of the conventional Pt/C catalyst (Figure 9).

## 4.2 Heteroatom-doped nonprecious transition metals

Furthermore, to improve the electrocatalytic activity of heteroatom-doped carbon materials, nonprecious transition metals such as manganese (Mn), iron (Fe), nickel (Ni), and cobalt (Co) could be incorporated into metal-free materials (Wu et al. 2011, Fu et al. 2015). Literature shows that nonprecious metal electrocatalysts exhibit higher catalytic activity and durability for ORR in alkaline electrolytes when compared to Pt-based catalysts. Nevertheless, the activity of these electrocatalysts needs tremendous improvement in acidic solutions (Wu et al. 2011, Kramm et al. 2014). Therefore, rational design of metal-incorporated, heteroatom-doped carbon materials that are active and stable for electrocatalytic reaction in acidic electrolytes is worthy of investigation. Heteroatom-doped carbon material will help mitigate the leaching of metal particles in the materials by inducing the formation of M-N-C bonds, thereby enhancing the catalyst activity and tolerance to carbonaceous species like  $\text{CO}$  and  $\text{CH}_3\text{OH}$  (Peera et al. 2016). Peera et al. (2016) investigated the incorporation of Fe and Co on N and F co-doped graphite nanofiber (Fe-Co/NF-GNF) during ORR in 0.5 M  $\text{HClO}_4$  solution. They found that Fe-Co/NF-GNF was remarkably durable toward ORR with a negative shift of about 10 mV in its half-wave potential at the end of 10,000 cycles, whereas commercial Pt/C showed a negative shift of about 200 mV under similar conditions. Rationally designed heteroatom-doped nonprecious transition metals can be utilized as bifunctional electrocatalysts, being suitable for both anodic and cathodic reactions. Yue et al. (2017) transformed tantalum dioxyfluoride ( $\text{TaO}_2\text{F}$ ) and graphitized carbon ( $^{\text{s}}\text{C}$ ) to an electrocatalyst ( $\text{TaO}_2\text{F}/^{\text{s}}\text{C}$ ) and tested its performance during OER under alkaline condition. The resulting electrocatalyst demonstrated an unusual activity with the



lower onset potential of 1.48 V vs. RHE and 360 mV overpotential to obtain a current density of 10 mA cm<sup>-2</sup>. At the same current density, TaO<sub>2</sub>F/<sup>8</sup>C demonstrated remarkable stability so that there was no significant change in the polarization curve even after 20,000 cycles.

## 5 Conclusion

Although carbide-supported Pt (Pt/C) has been considered as the best catalyst for GEOR, the major drawbacks of the Pt-based electrode include susceptibility to methanol crossover, time-dependent drift, and deactivation due to poisoning by intermediate carbon species such as formate and CO. Moreover, Pt-based catalysts are expensive and scarce, making them unsustainable for the commercial conversion of glycerol and fuel cell applications. Development of alternative anode electrocatalysts with better performance, as well as selectivity, which would enable complete glycerol electrooxidation to CO<sub>2</sub> at low overpotentials, is vital for efficient and cost-effective glycerol conversion. The anode catalyst must exhibit high activity toward C-C bond cleavage and must be resistant to poisoning by carbonaceous intermediate species. Generally, the catalytic performance of the material greatly depends on the catalyst's composition, microstructure, and morphology. One of the strategies employed to overcome these drawbacks is to lower the consumption of Pt either by substituting the Pt catalysts partially or totally using a proper support or by the nonprecious metal catalysts for the anodic reaction.

One way to reduce the consumption of Pt is to modify it with adatoms such as Sb, Sn, In, Bi, and Pb. This has helped in redirecting the electrooxidation pathway of Pt-based catalysts toward the production of value-added compounds such as DHA, tartronate, and mesoxalate. Modification with adatoms favors C-C cleavage to produce C<sub>1</sub> and C<sub>2</sub> products at high anode potentials. Moreover, incorporation of supports such as SiO<sub>2</sub>, CeO<sub>2-x</sub>, and graphene oxide (GO) can help reduce the amount of metal loading as well as enhance their stability, electrocatalytic activity, and utilization efficiency. Pd-based catalysts are also promising since Pd is more plentiful and cheaper than Pt. The electrochemical performance of Pd largely depends on its structure and can also be enhanced by modification with adatoms. Pd-based catalysts favor different selective reaction pathways (intermediates) and can produce CO<sub>2</sub> at high potentials, hydroxypyruvate at moderate potentials, and ketone and aldehyde at low potentials, indicating that product distribution depends

solely on the anode potential. Pd can also be promoted with metal oxides such as CeO<sub>2</sub>, TiO<sub>2</sub>, Mn<sub>3</sub>O<sub>4</sub>, Co<sub>3</sub>O<sub>4</sub>, and NiO toward remarkable electrocatalytic performance.

Gold-based catalysts are also a suitable substitute for Pt-based catalysts since they are less expensive. Au-based catalysts promote GEOR in alkaline electrolytes without susceptibility to poisoning by carbonaceous intermediate species due to their ability to adsorb a OH monolayer and force some of the reactor content to interact with water to form CO<sub>2</sub>. However, Au exhibits low activity for the oxidation of organics in acidic electrolytes. Ni-based catalysts are suitable candidates for the GEOR because they show high electrocatalytic activity, durability in alkaline solutions, and anti-poison ability. Rational incorporation of two or more transition metals as co-catalysts to obtain an enhanced geometric and electronic framework can considerably reduce the amount of Pt without penalizing the activity.

To further make glycerol electrooxidation cheaper, heteroatom-doped metal-free electrocatalysts are proposed. Heteroatom (N, B, S, P, F, I, Br, Cl) doping on carbon materials such as CNTs, graphene, activated carbon, and graphite can induce variation in spin densities and electronic charge densities in the carbon matrix, disturbing the electroneutrality and creating many catalytically active sites suitable for electrochemical reactions. Prominent among all the heteroatoms are nitrogen and fluorine, individually doped or co-doped. Co-doping offers a synergistic advantage. The electrocatalytic activity of heteroatom-doped carbon materials could be improved by incorporating nonprecious transition metals such as Mn, Fe, Ni, and Co. However, it is essential to ensure the rational design of an electrocatalyst from these materials to ensure suitability in acidic electrolytes.

**Acknowledgment:** The authors acknowledge the Fundamental Research Grant Scheme (FRGS) from the University of Malaya for funding this work through project no. FP046-2017A.

## References

- Abdel-Rahman MA, Tashiro Y, Sonomoto K. Lactic acid production from lignocellulose-derived sugars using lactic acid bacteria: overview and limits. *J Biotechnol* 2011; 156: 286–301.
- Akula S, Parthiban V, Peera SG, Singh B, Dhakate S, Sahu A. Simultaneous Co-doping of nitrogen and fluorine into MWCNTs: an in-situ conversion to graphene like sheets and its electro-catalytic activity toward oxygen reduction reaction. *J Electrochem Soc* 2017; 164: F568–F576.
- Akula S, Sahu A. Heteroatoms co-doping (N, F) to the porous carbon derived from spent coffee grounds as an effective catalyst for



- oxygen reduction reaction in polymer electrolyte fuel cells. *J Electrochem Soc* 2019; 166: F93–F101.
- Aliaga C, Park JY, Yamada Y, Lee HS, Tsung C-K, Yang P, Somorjai GA. Sum frequency generation and catalytic reaction studies of the removal of organic capping agents from Pt nanoparticles by UV–ozone treatment. *J Phys Chem C* 2009; 113: 6150–6155.
- Alsabet M, Grdeň M, Jerkiewicz G. Electrochemical growth of surface oxides on nickel. Part 3: Formation of  $\beta$ -NiOOH in relation to the polarization potential, polarization time, and temperature. *Electrocatalysis* 2015; 6: 60–71.
- Ashok A, Kumar A, Ponraj J, Mansour SA, Tarlochan F. Single step synthesis of porous NiCoO<sub>2</sub> for effective electrooxidation of glycerol in alkaline medium. *J Electrochem Soc* 2018; 165: J3301–J3309.
- Ashok A, Kumar A, Ponraj J, Mansour SA, Tarlochan F. Highly active and stable bi-functional NiCoO<sub>2</sub> catalyst for oxygen reduction and oxygen evolution reactions in alkaline medium. *Int J Hydrogen Energy* 2019; 44: 16603–16614.
- Aslam N, Masdar M, Kamarudin S, Daud W. Overview on direct formic acid fuel cells (DFACs) as an energy sources. *APCBEE Procedia* 2012; 3: 33–39.
- Avramov-Ivić M, Jovanović V, Vlajnić G, Pović J. The electrocatalytic properties of the oxides of noble metals in the electro-oxidation of some organic molecules. *J Electroanal Chem* 1997; 423: 119–124.
- Awasthi R, Singh R. Optimization of the Pd–Sn–GNS nanocomposite for enhanced electrooxidation of methanol. *Int J Hydrogen Energy* 2012; 37: 2103–2110.
- Bagheri S, Julkapli NM, Yehye WA. Catalytic conversion of biodiesel derived raw glycerol to value added products. *Renew Sustain Energy Rev* 2015; 41: 113–127.
- Bambagioni V, Bianchini C, Marchionni A, Filippi J, Vizza F, Teddy J, Serp P, Zhiani M. Pd and Pt–Ru anode electrocatalysts supported on multi-walled carbon nanotubes and their use in passive and active direct alcohol fuel cells with an anion-exchange membrane (alcohol = methanol, ethanol, glycerol). *J Power Sources* 2009; 190: 241–251.
- Baranova EA, Cally A, Allagui A, Ntais S, Wüthrich R. Nickel particles with increased catalytic activity towards hydrogen evolution reaction. *C R Chim* 2013; 16: 28–33.
- Bauer R, Hekmat D. Development of a transient segregated mathematical model of the semicontinuous microbial production process of dihydroxyacetone. *Biotechnol Prog* 2006; 22: 278–284.
- Bayatsarmadi B, Zheng Y, Jaroniec M, Qiao SZ. Soft-templating synthesis of N-doped mesoporous carbon nanospheres for enhanced oxygen reduction reaction. *Chem–Asian J* 2015; 10: 1546–1553.
- Behr A, Eilting J, Irawadi K, Leschinski J, Lindner F. Improved utilisation of renewable resources: new important derivatives of glycerol. *Green Chem* 2008; 10: 13–30.
- Benipal N, Qi J, Liu Q, Li W. Carbon nanotube supported PdAg nanoparticles for electrocatalytic oxidation of glycerol in anion exchange membrane fuel cells. *Appl Catal B* 2017; 210: 121–130.
- Benipal N, Qi J, Mcsweeney RF, Liang C, Li W. Electrocatalytic oxidation of meso-erythritol in anion-exchange membrane alkaline fuel cell on PdAg/CNT catalyst. *J Power Sources* 2018; 375: 345–350.
- Bijvoet J, Peerdeman A, Van Bommel A. Determination of the absolute configuration of optically active compounds by means of X-rays. *Nature* 1951; 168: 271.
- Brouzgou A, Song S, Tsiakaras P. Carbon-supported PdSn and Pd<sub>3</sub>Sn<sub>2</sub> anodes for glucose electrooxidation in alkaline media. *Appl Catal B* 2014; 158: 209–216.
- Cai J, Huang Y, Guo YJEA. Bi-modified Pd/C catalyst via irreversible adsorption and its catalytic activity for ethanol oxidation in alkaline medium. *Electrochim Acta* 2013; 99: 22–29.
- Caliman CC, Palma L, Ribeiro J. Evaluation of Ni and Ti addition in PtSn/C catalysts for ethanol and glycerol electrooxidation. *J Electrochem Soc* 2013; 160: F853–F858.
- Caneppele GL, Almeida TS, Zanata CR, Teixeira-Neto É, Fernández PS, Camara GA, Martins CA. Exponential improving in the activity of Pt/C nanoparticles towards glycerol electrooxidation by Sb ad-atoms deposition. *Appl Catal B* 2017; 200: 114–120.
- Carrettin S, Mcmorn P, Johnston P, Griffin K, Hutchings GJ. Selective oxidation of glycerol to glyceric acid using a gold catalyst in aqueous sodium hydroxide. *Chem Commun* 2002: 696–697.
- Carrettin S, Mcmorn P, Johnston P, Griffin K, Kiely CJ, Hutchings GJ. Oxidation of glycerol using supported Pt, Pd and Au catalysts. *Phys Chem Chem Phys* 2003; 5: 1329–1336.
- Chen Z, Higgins D, Tao H, Hsu RS, Chen Z. Highly active nitrogen-doped carbon nanotubes for oxygen reduction reaction in fuel cell applications. *J Phys Chem C* 2009; 113: 21008–21013.
- Chen L, Cui X, Wang Y, Wang M, Qiu R, Shu Z, Zhang L, Hua Z, Cui F, Weia C, Shi J. One-step synthesis of sulfur doped graphene foam for oxygen reduction reactions. *Dalton Trans* 2014; 43: 3420–3423.
- Chen W, Zhou Y, Shen Y. Product distribution of glycerol electro-oxidation over platinum-ceria/graphene nanosheet. *Electrochemistry* 2019; 87: 30–34.
- Chowdhury SR, Mukherjee P, Kumar Bhattacharya S. Palladium and palladium–copper alloy nano particles as superior catalyst for electrochemical oxidation of methanol for fuel cell applications. *Int J Hydrogen Energy* 2016; 41: 17072–17083.
- Ciriminna R, Pagliaro M. One-pot homogeneous and heterogeneous oxidation of glycerol to ketomalonic acid mediated by TEMPO. *Adv Synth Catal* 2003; 345: 383–388.
- Corma A, Iborra S, Velty A. Chemical routes for the transformation of biomass into chemicals. *Chem Rev* 2007; 107: 2411–2502.
- Cortright RD, Davda R, Dumesic JA. Hydrogen from catalytic reforming of biomass-derived hydrocarbons in liquid water. In: Dusastre V, editor. *Materials for sustainable energy: a collection of peer-reviewed research and review articles from Nature Publishing Group*. Singapore: World Scientific, 2011: 289–292.
- Das D, Das K. Cobalt hydroxide film on Pt as co-catalyst for oxidation of polyhydric alcohols in alkaline medium. *Mater Chem Phys* 2010; 123: 719–722.
- Dash S, Munichandraiah N. Nanoflowers of PdRu on PEDOT for electrooxidation of glycerol and its analysis. *Electrochim Acta* 2015; 180: 339–352.
- De Souza NE, Gomes JF, Tremiliosi-Filho G. Reactivity of 3-carbon-atom chain alcohols on gold electrode: a comparison to understand the glycerol electro-oxidation. *J Electroanal Chem* 2017; 800: 106–113.
- Denis PA. Band gap opening of monolayer and bilayer graphene doped with aluminium, silicon, phosphorus, and sulfur. *Chem Phys Lett* 2010; 492: 251–257.

- Denis PA. Concentration dependence of the band gaps of phosphorus and sulfur doped graphene. *Comput Mater Sci* 2013; 67: 203–206.
- Dibb JE, Arsenault M. Shouldn't snowpacks be sources of monocarboxylic acids? *Atmos Environ* 2002; 36: 2513–2522.
- Dodekatos G, SchüNemann S, Tüysüz H. Recent advances in thermo-, photo-, and electrocatalytic glycerol oxidation. *ACS Catal* 2018; 8: 6301–6333.
- Erini N, Loukrakpam R, Petkov V, Baranova EA, Yang R, Teschner D, Huang Y, Brankovic SR, Strasser P. Ethanol electro-oxidation on ternary platinum–rhodium–tin nanocatalysts: Insights in the atomic 3D structure of the active catalytic phase. *ACS Catal* 2014; 4: 1859–1867.
- Ernst S, Aldous L, Compton RG. The electrochemical reduction of oxygen at boron-doped diamond and glassy carbon electrodes: a comparative study in a room-temperature ionic liquid. *J Electroanal Chem* 2011; 663: 108–112.
- Falase A, Main M, Garcia K, Serov A, Lau C, Atanassov P. Electrooxidation of ethylene glycol and glycerol by platinum-based binary and ternary nano-structured catalysts. *Electrochim Acta* 2012; 66: 295–301.
- Faro ML, Minutoli M, Monforte G, Antonucci V, Aricò AS. Glycerol oxidation in solid oxide fuel cells based on a Ni-perovskite electrocatalyst. *Biomass Bioenergy* 2011; 35: 1075–1084.
- Fashedemi OO, Miller HA, Marchionni A, Vizza F, Ozoemena KI. Electro-oxidation of ethylene glycol and glycerol at palladium-decorated FeCo@ Fe core–shell nanocatalysts for alkaline direct alcohol fuel cells: functionalized MWCNT supports and impact on product selectivity. *J Mater Chem A* 2015; 3: 7145–7156.
- Fernández PS, Martins ME, Camara GA. New insights about the electro-oxidation of glycerol on platinum nanoparticles supported on multi-walled carbon nanotubes. *Electrochim Acta* 2012a; 66: 180–187.
- Fernández PS, Martins ME, Martins CA, Camara GA. The electro-oxidation of isotopically labeled glycerol on platinum: new information on C–C bond cleavage and CO<sub>2</sub> production. *Electrochem Commun* 2012b; 15: 14–17.
- Fernández PS, Martins CA, Martins ME, Camara GA. Electrooxidation of glycerol on platinum nanoparticles: deciphering how the position of each carbon affects the oxidation pathways. *Electrochim Acta* 2013; 112: 686–691.
- Ferreira Jr RS, Giz MJ, Camara GA. Influence of the local pH on the electrooxidation of glycerol on Palladium–Rhodium electrodeposits. *J Electroanal Chem* 2013; 697: 15–20.
- Fornaro A, Gutz IG. Wet deposition and related atmospheric chemistry in the São Paulo metropolis, Brazil: Part 2 – contribution of formic and acetic acids. *Atmos Environ* 2003; 37: 117–128.
- Freitas M. Nickel hydroxide powder for NiO · OH/Ni (OH) 2 electrodes of the alkaline batteries. *J Power Sources* 2001; 93: 163–173.
- Frota Jr EF, De Barros VVS, De Araújo BR, Purgatto ÂG, Linares JJ. Pt/C containing different platinum loadings for use as electrocatalysts in alkaline PBI-based direct glycerol fuel cells. *Int J Hydrogen Energy* 2017; 42: 23095–23106.
- Fu S, Zhu C, Li H, Du D, Lin Y. One-step synthesis of cobalt and nitrogen co-doped carbon nanotubes and their catalytic activity for the oxygen reduction reaction. *J Mater Chem A* 2015; 3: 12718–12722.
- Gao S, Li L, Geng K, Wei X, Zhang S. Recycling the biowaste to produce nitrogen and sulfur self-doped porous carbon as an efficient catalyst for oxygen reduction reaction. *Nano Energy* 2015; 16: 408–418.
- Garcia AG, Lopes PP, Gomes JF, Pires C, Ferreira EB, Lucena RG, Gasparotto LHS, Tremiliosi-Filho G. Eco-friendly synthesis of bimetallic AuAg nanoparticles. *New J Chem* 2014; 38: 2865–2873.
- Garcia AC, Caliman J, Ferreira EB, Tremiliosi-Filho G, Linares JJ. Promotional effect of Ag on the catalytic activity of Au for glycerol electrooxidation in alkaline medium. *ChemElectroChem* 2015; 2: 1036–1041.
- Garcia AC, Kolb MJ, Van Nierop Y, Sanchez C, Vos J, Birdja YY, Kwon Y, Tremiliosi-Filho G, Koper MTM. Strong impact of platinum surface structure on primary and secondary alcohol oxidation during electro-oxidation of glycerol. *ACS Catal* 2016; 6: 4491–4500.
- Garcia AC, Birdja YY, Tremiliosi-Filho G, Koper MT. Glycerol electro-oxidation on bismuth-modified platinum single crystals. *J Catal* 2017; 346: 117–124.
- Gomes JF, Tremiliosi-Filho G. Spectroscopic studies of the glycerol electro-oxidation on polycrystalline Au and Pt surfaces in acidic and alkaline media. *Electrocatalysis* 2011; 2: 96.
- Gomes JF, Martins CA, Giz MJ, Tremiliosi-Filho G, Camara GA. Insights into the adsorption and electro-oxidation of glycerol: self-inhibition and concentration effects. *J Catal* 2013; 301: 154–161.
- Gomes J, Garcia A, Gasparotto L, De Souza N, Ferreira E, Pires C, Tremiliosi-Filho G. Influence of silver on the glycerol electro-oxidation over AuAg/C catalysts in alkaline medium: a cyclic voltammetry and in situ FTIR spectroscopy study. *Electrochim Acta* 2014a; 144: 361–368.
- Gomes JF, Garcia AC, Pires C, Ferreira EB, Albuquerque RQ, Tremiliosi-Filho G, Gasparotto LHS. Impact of the AuAg NPs composition on their structure and properties: a theoretical and experimental investigation. *J Phys Chem C* 2014b; 118: 28868–28875.
- Gong K, Du F, Xia Z, Durstock M, Dai L. Nitrogen-doped carbon nanotube arrays with high electrocatalytic activity for oxygen reduction. *Science* 2009; 323: 760–764.
- Greiner MT, Helander MG, Tang W-M, Wang Z-B, Qiu J, Lu Z-H. Universal energy-level alignment of molecules on metal oxides. *Nat Mater* 2012; 11: 76.
- Guerra-Balcázar M, Morales-Acosta D, Castaneda F, Ledesma-García J, Arriaga L. Synthesis of Au/C and Au/PANI for anode electrodes in glucose microfluidic fuel cell. *Electrochem Commun* 2010; 12: 864–867.
- Guima K-E, Alencar LM, Da Silva GC, Trindade MA, Martins CA. 3D-printed electrolyzer for the conversion of glycerol into tartronate on Pd nanocubes. *ACS Sustain Chem Eng* 2017; 6: 1202–1207.
- Habibi E, Razmi H. Glycerol electrooxidation on Pd, Pt and Au nanoparticles supported on carbon ceramic electrode in alkaline media. *Int J Hydrogen Energy* 2012; 37: 16800–16809.
- Hajar YM, Houache MS, Tariq U, Vernoux P, Baranova EA. Nanoscopic Ni interfaced with oxygen conductive supports: link between electrochemical and catalytic studies. *ECS Trans* 2017; 77: 51–66.
- Han J, Kim Y, Kim HW, Jackson DH, Lee D, Chang H, Chae HJ, Lee KY, Kim HJ. Effect of atomic-layer-deposited TiO<sub>2</sub> on carbon-

- supported Ni catalysts for electrocatalytic glycerol oxidation in alkaline media. *Electrochem Commun* 2017; 83: 46–50.
- Han J, Kim Y, Jackson DH, Jeong K-E, Chae H-J, Lee K-Y, Kim HJ. Role of Au-TiO<sub>2</sub> interfacial sites in enhancing the electrocatalytic glycerol oxidation performance. *Electrochem Commun* 2018; 96: 16–21.
- He W, Jiang C, Wang J, Lu L. High-rate oxygen electroreduction over graphitic-N species exposed on 3D hierarchically porous nitrogen-doped carbons. *Angew Chem Int Ed* 2014; 53: 9503–9507.
- He Q, Shen Y, Xiao K, Xi J, Qiu X. Alcohol electro-oxidation on platinum–ceria/graphene nanosheet in alkaline solutions. *Int J Hydrogen Energy* 2016; 41: 20709–20719.
- Holade Y, Morais C, Arrii-Clacens S, Servat K, Napporn T, Kokoh K. New preparation of PdNi/C and PdAg/C nanocatalysts for glycerol electrooxidation in alkaline medium. *Electrocatalysis* 2013a; 4: 167–178.
- Holade Y, Morais CU, Servat K, Napporn TW, Kokoh KB. Toward the electrochemical valorization of glycerol: Fourier transform infrared spectroscopic and chromatographic studies. *ACS Catal* 2013b; 3: 2403–2411.
- Houache MS, Cossar E, Ntais S, Baranova EA. Electrochemical modification of nickel surfaces for efficient glycerol electrooxidation. *J Power Sources* 2018; 375: 310–319.
- Hoyt RA, Remillard EM, Cubuk ED, Vecitis CD, Kaxiras E. Polyiodide-doped graphene. *J Phys Chem C* 2016; 121: 609–615.
- Hu C, Wang X. Highly dispersed palladium nanoparticles on commercial carbon black with significantly high electrocatalytic activity for methanol and ethanol oxidation. *Int J Hydrogen Energy* 2015; 40: 12382–12391.
- Huan TN, Shinde DV, Kim S, Han S-H, Artero V, Chung H. Forest of Pt–Au–Ag tri-metallic nanodendrites as an efficient electrocatalyst for methanol oxidation reaction. *RSC Adv* 2015; 5: 6940–6944.
- Hurley RB. Process for production of a tartronic acid solution. In: Google Patents. 1982.
- Inoue H, Kimura S, Teraoka Y, Chiku M, Higuchi E, Lam BTX. Mechanism of glycerol oxidation reaction on silver-modified palladium electrode in alkaline medium. *Int J Hydrogen Energy* 2018; 43: 18664–18671.
- Israili ZH. Antimicrobial properties of honey. *Am J Ther* 2014; 21: 304–323.
- Jeffery DZ, Camara GA. The formation of carbon dioxide during glycerol electrooxidation in alkaline media: first spectroscopic evidences. *Electrochem Commun* 2010; 12: 1129–1132.
- Jeon I-Y, Choi H-J, Choi M, Seo J-M, Jung S-M, Kim M-J, Zhang S, Zhang L, Xia Z, Dai L, Park N, Baek JB. Facile, scalable synthesis of edge-halogenated graphene nanoplatelets as efficient metal-free electrocatalysts for oxygen reduction reaction. *Sci Rep* 2013; 3: 1810.
- Jin M, Zhang H, Xie Z, Xia Y. Palladium concave nanocubes with high-index facets and their enhanced catalytic properties. *Angew Chem Int Ed* 2011; 50: 7850–7854.
- Jin C, Sun X, Chen Z. Electrocatalytic oxidation of C3 alcohols on Au, Pt and Pt-modified Au electrodes. *Chem Eng Technol* 2012; 35: 1064–1068.
- Johnson DT, Taconi KA. The glycerin glut: options for the value-added conversion of crude glycerol resulting from biodiesel production. *Environ Prog* 2007; 26: 338–348.
- Kang Y, Wang W, Pu Y, Li J, Chai D, Lei Z. An effective Pd-NiO<sub>x</sub>-P composite catalyst for glycerol electrooxidation: co-existed phosphorus and nickel oxide to enhance performance of Pd. *Chem Eng J* 2017; 308: 419–427.
- Katryniok B, Kimura H, Skrzyńska E, Girardon J-S, Fongarland P, Capron M, Ducoulombier R, Mimura N, Paul S, Dumeignil F. Selective catalytic oxidation of glycerol: perspectives for high value chemicals. *Green Chem* 2011; 13: 1960–1979.
- Kim HJ, Choi SM, Green SK, Tompsett GA, Lee SH, Huber GW, Kim WB. Highly active and stable PtRuSn/C catalyst for electrooxidations of ethylene glycol and glycerol. *Appl Catal B* 2011a; 101: 366–375.
- Kim HJ, Choi SM, Seo MH, Green S, Huber GW, Kim WB. Efficient electrooxidation of biomass-derived glycerol over a graphene-supported PtRu electrocatalyst. *Electrochem Commun* 2011b; 13: 890–893.
- Kim Y, Kim H, Kim WB. PtAg nanotubes for electrooxidation of ethylene glycol and glycerol in alkaline media. *Electrochem Commun* 2014; 46: 36–39.
- Kim HJ, Kim Y, Lee D, Kim J-R, Chae H-J, Jeong S-Y, Kim B-S, Lee J, Huber GW, Byun J, Kim S, Han J. Coproducing value-added chemicals and hydrogen with electrocatalytic glycerol oxidation technology: experimental and techno-economic investigations. *ACS Sustain Chem Eng* 2017; 5: 6626–6634.
- Kimura H. Selective oxidation of glycerol on a platinum-bismuth catalyst by using a fixed bed reactor. *Appl Catal A* 1993; 105: 147–158.
- Kramm UI, Lefèvre M, Larouche N, Schmeisser D, Dodelet J-P. Correlations between mass activity and physicochemical properties of Fe/N/C catalysts for the ORR in PEM fuel cell via 57Fe Mossbauer spectroscopy and other techniques. *J Am Chem Soc* 2014; 136: 978–985.
- Kwon Y, Lai SC, Rodriguez P, Koper MT. Electrocatalytic oxidation of alcohols on gold in alkaline media: base or gold catalysis? *J Am Chem Soc* 2011a; 133: 6914–6917.
- Kwon Y, Schouten KJP, Koper MT. Mechanism of the catalytic oxidation of glycerol on polycrystalline gold and platinum electrodes. *ChemCatChem* 2011b; 3: 1176–1185.
- Kwon Y, Birdja Y, Spanos I, Rodriguez P, Koper MT. Highly selective electro-oxidation of glycerol to dihydroxyacetone on platinum in the presence of bismuth. *ACS Catal* 2012; 2: 759–764.
- Kwon Y, Hersbach TJ, Koper MT. Electro-oxidation of glycerol on platinum modified by adatoms: activity and selectivity effects. *Top Catal* 2014; 57: 1272–1276.
- Lee S, Kim HJ, Choi SM, Seo MH, Kim WB. The promotional effect of Ni on bimetallic PtNi/C catalysts for glycerol electrooxidation. *Appl Catal A* 2012; 429: 39–47.
- Lee S, Kim HJ, Lim EJ, Kim Y, Noh Y, Huber GW, Kim WB. Highly selective transformation of glycerol to dihydroxyacetone without using oxidants by a PtSb/C-catalyzed electrooxidation process. *Green Chem* 2016; 18: 2877–2887.
- Li Y, Zaera F. Sensitivity of the glycerol oxidation reaction to the size and shape of the platinum nanoparticles in Pt/SiO<sub>2</sub> catalysts. *J Catal* 2015; 326: 116–126.
- Li S-S, Hu Y-Y, Feng J-J, Lv Z-Y, Chen J-R, Wang A-J. Rapid room-temperature synthesis of Pd nanodendrites on reduced graphene oxide for catalytic oxidation of ethylene glycol and glycerol. *Int J Hydrogen Energy* 2014; 39: 3730–3738.
- Li F, Shu H, Liu X, Shi Z, Liang P, Chen X. Electrocatalytic activity and design principles of heteroatom-doped graphene catalysts for

- oxygen-reduction reaction. *J Phys Chem C* 2017; 121: 14434–14442.
- Liang J, Jiao Y, Jaroniec M, Qiao SZ. Sulfur and nitrogen dual-doped mesoporous graphene electrocatalyst for oxygen reduction with synergistically enhanced performance. *Angew Chem Int Ed* 2012; 51: 11496–11500.
- Liu Z, Peng F, Wang H, Yu H, Tan J, Zhu L. Novel phosphorus-doped multiwalled nanotubes with high electrocatalytic activity for O<sub>2</sub> reduction in alkaline medium. *Catal Commun* 2011; 16: 35–38.
- Liu Z, Peng F, Wang H, Yu H, Zheng W, Wei X. Preparation of phosphorus-doped carbon nanospheres and their electrocatalytic performance for O<sub>2</sub> reduction. *J Nat Gas Chem* 2012; 21: 257–264.
- Liu X, Fu G, Chen Y, Tang Y, She P, Lu T. Pt-Pd-Co trimetallic alloy network nanostructures with superior electrocatalytic activity towards the oxygen reduction reaction. *Chem-Eur J* 2014; 20: 585–590.
- Liu J, Song P, Ning Z, Xu W. Recent advances in heteroatom-doped metal-free electrocatalysts for highly efficient oxygen reduction reaction. *Electrocatalysis* 2015; 6: 132–147.
- Liu R, Zhang H, Liu S, Zhang X, Wu T, Ge X, Zang Y, Zhao H, Wang G. Shrimp-shell derived carbon nanodots as carbon and nitrogen sources to fabricate three-dimensional N-doped porous carbon electrocatalysts for the oxygen reduction reaction. *Phys Chem Chem Phys* 2016; 18: 4095–4101.
- Liu D, Fu L, Huang X, Liu K, Li J, Xie H, Wang H, Tang Y. Influence of iron source type on the electrocatalytic activity toward oxygen reduction reaction in Fe-N/C for Al-air batteries. *J Electrochem Soc* 2018a; 165: F662–F670.
- Liu Y, Yu W, Raciti D, Gracias DH, Wang C. Electrocatalytic oxidation of glycerol on platinum. *J Phys Chem C* 2018b; 123: 426–432.
- Loeffler KW, Koehler CA, Paul NM, De Haan DO. Oligomer formation in evaporating aqueous glyoxal and methyl glyoxal solutions. *Environ Sci Technol* 2006; 40: 6318–6323.
- Machado BF, Marchionni A, Bacsa RR, Bellini M, Beausoleil J, Oberhauser W, Vizza F, Serp P. Synergistic effect between few layer graphene and carbon nanotube supports for palladium catalyzing electrochemical oxidation of alcohols. *J Energy Chem* 2013; 22: 296–304.
- Maillard F, Savinova ER, Simonov PA, Zaikovskii VI, Stimming U. Infrared spectroscopic study of CO adsorption and electro-oxidation on carbon-supported Pt nanoparticles: interparticle versus intraparticle heterogeneity. *J Phys Chem B* 2004; 108: 17893–17904.
- Mamtani K, Ozkan US. Heteroatom-doped carbon nanostructures as oxygen reduction reaction catalysts in acidic media: an overview. *Catal Lett* 2015; 145: 436–450.
- Morrison AR, Hosseiny SS, Wüthrich R. Platinum-like oxidation of nickel surfaces by rapidly switching voltage to generate highly active bifunctional catalysts. *Electrochem Commun* 2016; 67: 22–25.
- Mamtani K, Jain D, Dogu D, Gustin V, Gunduz S, Co AC, Ozkan US. Insights into oxygen reduction reaction (ORR) and oxygen evolution reaction (OER) active sites for nitrogen-doped carbon nanostructures (CN<sub>x</sub>) in acidic media. *Appl Catal B* 2018; 220: 88–97.
- Mougenot M, Caillard A, Simoes M, Baranton S, Coutanceau C, Brault P. PdAu/C catalysts prepared by plasma sputtering for the electro-oxidation of glycerol. *Appl Catal B* 2011; 107: 372–379.
- Nam K-W, Yoon W-S, Kim K-B. X-ray absorption spectroscopy studies of nickel oxide thin film electrodes for supercapacitors. *Electrochim Acta* 2002; 47: 3201–3209.
- Niu Z, Li Y. Removal and utilization of capping agents in nanocatalysis. *Chem Mater* 2013; 26: 72–83.
- Oliveira V, Morais C, Servat K, Napporn T, Tremiliosi-Filho G, Kokoh KB. Glycerol oxidation on nickel based nanocatalysts in alkaline medium—identification of the reaction products. *J Electroanal Chem* 2013; 703: 56–62.
- Oliveira V, Morais C, Servat K, Napporn T, Tremiliosi-Filho G, Kokoh K. Studies of the reaction products resulted from glycerol electrooxidation on Ni-based materials in alkaline medium. *Electrochim Acta* 2014; 117: 255–262.
- Oliveira V, Morais C, Servat K, Napporn T, Olivi P, Kokoh KB, Tremiliosi-Filho G. Kinetic investigations of glycerol oxidation reaction on Ni/C. *Electrocatalysis* 2015; 6: 447–454.
- Önal A. Overview on liquid chromatographic analysis of tetracycline residues in food matrices. *Food Chem* 2011; 127: 197–203.
- Ozaki J-I. Simultaneous doping of boron and nitrogen into a carbon to enhance its oxygen reduction activity in proton exchange membrane fuel cells. *Carbon* 2006; 44: 3358.
- Painter RM, Pearson DM, Waymouth RM. Selective catalytic oxidation of glycerol to dihydroxyacetone. *Angew Chem Int Ed* 2010; 49: 9456–9459.
- Peera SG, Sahu A, Arunchander A, Bhat S, Karthikeyan J, Murugan P. Nitrogen and fluorine co-doped graphite nanofibers as high durable oxygen reduction catalyst in acidic media for polymer electrolyte fuel cells. *Carbon* 2015; 93: 130–142.
- Peera SG, Arunchander A, Sahu A. Cumulative effect of transition metals on nitrogen and fluorine co-doped graphite nanofibers: an efficient and highly durable non-precious metal catalyst for the oxygen reduction reaction. *Nanoscale* 2016; 8: 14650–14664.
- Pinter JK, Hayashi JA, Watson JA. Enzymic assay of glycerol, dihydroxyacetone, and glyceraldehyde. *Arch Biochem Biophys* 1967; 121: 404–414.
- Qi J, Xin L, Chadderdon DJ, Qiu Y, Jiang Y, Benipal N, Liang C, Li W. Electrocatalytic selective oxidation of glycerol to tartronate on Au/C anode catalysts in anion exchange membrane fuel cells with electricity cogeneration. *Appl Catal B* 2014; 154: 360–368.
- Qi J, Benipal N, Liang C, Li W. PdAg/CNT catalyzed alcohol oxidation reaction for high-performance anion exchange membrane direct alcohol fuel cell (alcohol= methanol, ethanol, ethylene glycol and glycerol). *Appl Catal B* 2016; 199: 494–503.
- Ramulifho T, Ozoemena KI, Modibedi RM, Jafta CJ, Mathe MK. Electrocatalytic oxidation of ethylene glycol at palladium-bimetallic nanocatalysts (PdSn and PdNi) supported on sulfonate-functionalised multi-walled carbon nanotubes. *J Electroanal Chem* 2013; 692: 26–30.
- Reier T, Oezaslan M, Strasser P. Electrocatalytic oxygen evolution reaction (OER) on Ru, Ir, and Pt catalysts: a comparative study of nanoparticles and bulk materials. *ACS Catal* 2012; 2: 1765–1772.
- Rezaei B, Havakeshian E, Ensafi AA. Fabrication of a porous Pd film on nanoporous stainless steel using galvanic replacement as a novel electrocatalyst/electrode design for glycerol oxidation. *Electrochim Acta* 2014; 136: 89–96.
- Rezaei B, Saeidi-Boroujeni S, Havakeshian E, Ensafi AA. Highly efficient electrocatalytic oxidation of glycerol by Pt-Pd/Cu trimetallic nanostructure electrocatalyst supported



- on nanoporous stainless steel electrode using galvanic replacement. *Electrochim Acta* 2016; 203: 41–50.
- Roquet L, Belgsir E, Léger J-M, Lamy C. Kinetics and mechanisms of the electrocatalytic oxidation of glycerol as investigated by chromatographic analysis of the reaction products: potential and pH effects. *Electrochim Acta* 1994; 39: 2387–2394.
- Rostami H, Omrani A, Rostami AA. On the role of electrodeposited nanostructured Pd–Co alloy on Au for the electrocatalytic oxidation of glycerol in alkaline media. *Int J Hydrogen Energy* 2015; 40: 9444–9451.
- Rostami H, Abdollahi T, Mehdipour P, Rostami AA, Farmanzadeh D. Effect of Ni addition on electrocatalytic activity of PdCu catalysts for ethanol electrooxidation: an experimental and theoretical study. *Int J Hydrogen Energy* 2017; 42: 24713–24725.
- Sah AK, Verma VK. Syzygium cumini: an overview. *J Chem Pharm Res* 2011; 3: 108–113.
- Sandrini RM, Sempionatto JR, Herrero E, Feliu JM, Souza-Garcia J, Angelucci CA. Mechanistic aspects of glycerol electrooxidation on Pt (111) electrode in alkaline media. *Electrochem Commun* 2018; 86: 149–152.
- Sankar M, Dimitratos N, Knight DW, Carley AF, Tiruvalam R, Kiely CJ, Thomas D, Hutchings GJ. Oxidation of glycerol to glycolate by using supported gold and palladium nanoparticles. *ChemSusChem* 2009; 2: 1145–1151.
- Santos D, Sequeira C. Cyclic voltammetry investigation of borohydride oxidation at a gold electrode. *Electrochim Acta* 2010; 55: 6775–6781.
- Schmidt T, Behm R, Grgur B, Markovic N, Ross P. Formic acid oxidation on pure and Bi-modified Pt (111): temperature effects. *Langmuir* 2000; 16: 8159–8166.
- Schnaidt J, Heinen M, Denot D, Jusys Z, Behm RJ. Electrooxidation of glycerol studied by combined in situ IR spectroscopy and online mass spectrometry under continuous flow conditions. *J Electroanal Chem* 2011; 661: 250–264.
- Shen S, Zhao T, Xu J, Li Y. Synthesis of PdNi catalysts for the oxidation of ethanol in alkaline direct ethanol fuel cells. *J Power Sources* 2010; 195: 1001–1006.
- Sheng Z-H, Gao H-L, Bao W-J, Wang F-B, Xia X-H. Synthesis of boron doped graphene for oxygen reduction reaction in fuel cells. *J Mater Chem A* 2012; 22: 390–395.
- Silva LS, López-Suárez FE, Perez-Cadenas M, Santos SF, Da Costa LP, Eguiluz KI, Salazar-Banda GR. Synthesis and characterization of highly active Pbx@Pty/C core-shell nanoparticles toward glycerol electrooxidation. *Appl Catal B* 2016; 198: 38–48.
- Silva JCM, Assumpção MH, Hammer P, Neto AO, Spinacé EV, Baranova EA. Iridium – rhodium nanoparticles for ammonia oxidation: electrochemical and fuel cell studies. *ChemElectroChem* 2017; 4: 1101–1107.
- Simões M, Baranton S, Coutanceau C. Electro-oxidation of glycerol at Pd based nano-catalysts for an application in alkaline fuel cells for chemicals and energy cogeneration. *Appl Catal B* 2010; 93: 354–362.
- Simões M, Baranton S, Coutanceau C. Enhancement of catalytic properties for glycerol electrooxidation on Pt and Pd nanoparticles induced by Bi surface modification. *Appl Catal B* 2011; 110: 40–49.
- Simões M, Baranton S, Coutanceau C. Electrochemical valorisation of glycerol. *ChemSusChem* 2012; 5: 2106–2124.
- Simoneit BR. Prebiotic organic synthesis under hydrothermal conditions: an overview. *Adv Space Res* 2004; 33: 88–94.
- Singh R, Singh A. Electrocatalytic activities of binary and ternary composite electrodes of Pd, nanocarbon and Ni for electro-oxidation of methanol in alkaline medium. *J Solid State Electrochem* 2009; 13: 1259–1265.
- Song MY, Yang D-S, Singh KP, Yuan J, Yu J-S. Nitrogen-doped hollow carbon spheres with highly graphitized mesoporous shell: role of Fe for oxygen evolution reaction. *Appl Catal B* 2016; 191: 202–208.
- Staudt M, Wolf A, Kesselmeier J. Influence of environmental factors on the emissions of gaseous formic and acetic acids from orange (*Citrus sinensis* L.) foliage. *Biogeochemistry* 2000; 48: 199–216.
- Strelko V, Kuts V, Thrower P. On the mechanism of possible influence of heteroatoms of nitrogen, boron and phosphorus in a carbon matrix on the catalytic activity of carbons in electron transfer reactions. *Carbon* 2000; 10: 1499–1503.
- Su L, Jia W, Schempf A, Lei Y. Palladium/titanium dioxide nanofibers for glycerol electrooxidation in alkaline medium. *Electrochem Commun* 2009; 11: 2199–2202.
- Sun X, Song P, Chen T, Liu J, Xu W. Fluorine-doped BP 2000: highly efficient metal-free electrocatalysts for acidic oxygen reduction reaction with superlow H<sub>2</sub>O<sub>2</sub> yield. *Chem Commun* 2013a; 49: 10296–10298.
- Sun X, Song P, Zhang Y, Liu C, Xu W, Xing W. A class of high performance metal-free oxygen reduction electrocatalysts based on cheap carbon blacks. *Sci Rep* 2013b; 3: 2505.
- Suzuki NY, Santiago PV, Galhardo TS, Carvalho WA, Souza-Garcia J, Angelucci CA. Insights of glycerol electrooxidation on polycrystalline silver electrode. *J Electroanal Chem* 2016; 780: 391–395.
- Tehrani RM, Ab Ghani S. Electrocatalysis of free glycerol at a nanonickel modified graphite electrode and its determination in biodiesel. *Electrochim Acta* 2012; 70: 153–157.
- Thia L, Xie M, Kim D, Wang X. Ag containing porous Au structures as highly selective catalysts for glycolate and formate. *Cataly Sci Technol* 2017; 7: 874–881.
- Vaidya A, Pandey R, Mudliar S, Kumar MS, Chakrabarti T, Devotta S. Production and recovery of lactic acid for polylactide – an overview. *Crit Rev Environ Sci Technol* 2005; 35: 429–467.
- Valter M, Busch M, Wickman BR, Grönbeck H, Baltusaitis J, Hellman A. Electrooxidation of glycerol on gold in acidic medium: a combined experimental and DFT study. *J Phys Chem C* 2018; 122: 10489–10494.
- Venancio E, Napporn W, Motheo A. Electro-oxidation of glycerol on platinum dispersed in polyaniline matrices. *Electrochim Acta* 2002; 47: 1495–1501.
- Wang Z, Hu F, Shen PK. Carbonized porous anodic alumina as electrocatalyst support for alcohol oxidation. *Electrochem Commun* 2006; 8: 1764–1768.
- Wang Y, Sheng ZM, Yang H, Jiang SP, Li CM. Electrocatalysis of carbon black-or activated carbon nanotubes-supported Pd–Ag towards methanol oxidation in alkaline media. *Int J Hydrogen Energy* 2010; 35: 10087–10093.
- Wang S, Iyyamperumal E, Roy A, Xue Y, Yu D, Dai L. Vertically aligned BCN nanotubes as efficient metal-free electrocatalysts for the oxygen reduction reaction: a synergetic effect by Co-doping with boron and nitrogen. *Angew Chem Int Ed* 2011; 50: 11756–11760.



- Wang H, Thia S L, Li N, Ge X, Liu Z, Wang X. Pd nanoparticles on carbon nitride-graphene for the selective electro-oxidation of glycerol in alkaline solution. *ACS Catal* 2015; 5: 3174–3180.
- Wang W, Kang Y, Yang Y, Liu Y, Chai D, Lei Z. PdSn alloy supported on phenanthroline-functionalized carbon as highly active electrocatalysts for glycerol oxidation. *Int J Hydrogen Energy* 2016; 41: 1272–1280.
- Wang W, Jing W, Wang F, Liu S, Liu X, Lei Z. Amorphous ultra-dispersed Pt clusters supported on nitrogen functionalized carbon: a superior electrocatalyst for glycerol electrooxidation. *J Power Sources* 2018; 399: 357–362.
- Wang C, Zhang K, Xu H, Du Y, Goh MC. Anchoring gold nanoparticles on poly (3, 4-ethylenedioxythiophene)(PEDOT) nanonet as three-dimensional electrocatalysts toward ethanol and 2-propanol oxidation. *J Colloid Interface Sci* 2019; 541: 258–268.
- Wesselmark M, Wickman B, Lagergren C, Lindbergh G. The impact of iridium on the stability of platinum on carbon thin-film model electrodes. *Electrochim Acta* 2013; 111: 152–159.
- Wu G, More KL, Johnston CM, Zelenay P. High-performance electrocatalysts for oxygen reduction derived from polyaniline, iron, and cobalt. *Science* 2011; 332: 443–447.
- Xin L, Zhang Z, Wang Z, Li W. Simultaneous generation of mesoxalic acid and electricity from glycerol on a gold anode catalyst in anion-exchange membrane fuel cells. *ChemCatChem* 2012; 4: 1105–1114.
- Xu Y, Zhang B. Recent advances in porous Pt-based nanostructures: synthesis and electrochemical applications. *Chem Soc Rev* 2014; 43: 2439–2450.
- Xu C, Tian Z, Shen P, Jiang SP. Oxide (CeO<sub>2</sub>, NiO, Co<sub>3</sub>O<sub>4</sub> and Mn<sub>3</sub>O<sub>4</sub>)-promoted Pd/C electrocatalysts for alcohol electrooxidation in alkaline media. *Electrochim Acta* 2008; 53: 2610–2618.
- Xu H, Yan B, Zhang K, Wang J, Li S, Wang C, Shiraishi Y, Du Y, Yang P. Ultrasonic-assisted synthesis of N-doped graphene-supported binary PdAu nanoflowers for enhanced electro-oxidation of ethylene glycol and glycerol. *Electrochim Acta* 2017; 245: 227–236.
- Xu H, Song P, Fernandez C, Wang J, Zhu M, Shiraishi Y, Du Y. Sophisticated construction of binary PdPb alloy nanocubes as robust electrocatalysts toward ethylene glycol and glycerol oxidation. *ACS Appl Mater Interfaces* 2018; 10: 12659–12665.
- Yadav RM, Wu J, Kochandra R, Ma L, Tiwary CS, Ge L, Ye G, Vajtai R, Lou J, Ajayan P. Carbon nitrogen nanotubes as efficient bifunctional electrocatalysts for oxygen reduction and evolution reactions. *ACS Appl Mater Interfaces* 2015; 7: 11991–12000.
- Yang L, Jiang S, Zhao Y, Zhu L, Chen S, Wang X, Wu Q, Ma J, Ma Y, Hu Z. Boron-doped carbon nanotubes as metal-free electrocatalysts for the oxygen reduction reaction. *Angew Chem Int Ed* 2011a; 50: 7132–7135.
- Yang Z, Nie H, Zhou X, Yao Z, Huang S, Chen X. Investigation of homologous series as precursory hydrocarbons for aligned carbon nanotube formation by the spray pyrolysis method. *Nano* 2011b; 6: 205–213.
- Yang Z, Yao Z, Li G, Fang G, Nie H, Liu Z, Zhou X, Chen X, Huang S. Sulfur-doped graphene as an efficient metal-free cathode catalyst for oxygen reduction. *ACS Nano* 2011c; 6: 205–211.
- Yang S, Zhi L, Tang K, Feng X, Maier J, Müllen K. Efficient synthesis of heteroatom (N or S)-doped graphene based on ultrathin graphene oxide-porous silica sheets for oxygen reduction reactions. *Adv Funct Mater* 2012; 22: 3634–3640.
- Yang W, Yue X, Liu X, Zhai J, Jia J. IL-derived N, S co-doped ordered mesoporous carbon for high-performance oxygen reduction. *Nanoscale* 2015; 7: 11956–11961.
- Yao Z, Nie H, Yang Z, Zhou X, Liu Z, Huang S. Catalyst-free synthesis of iodine-doped graphene via a facile thermal annealing process and its use for electrocatalytic oxygen reduction in an alkaline medium. *Chem Commun* 2012; 48: 1027–1029.
- Yu D, Xue Y, Dai L. Vertically aligned carbon nanotube arrays co-doped with phosphorus and nitrogen as efficient metal-free electrocatalysts for oxygen reduction. *J Phys Chem Lett* 2012; 3: 2863–2870.
- Yue X, Jin Y, Shen PK. Highly stable and efficient non-precious metal electrocatalysts of tantalum dioxide used for the oxygen evolution reaction. *J Mater Chem A* 2017; 5: 8287–8291.
- Zalineeva A, Baranton S, Coutanceau C. Bi-modified palladium nanocubes for glycerol electrooxidation. *Electrochim Commun* 2013; 34: 335–338.
- Zalineeva A, Serov A, Padilla M, Martinez U, Artyushkova K, Baranton SV, Coutanceau C, Atanassov PB. Self-supported Pd<sub>x</sub>Bi catalysts for the electrooxidation of glycerol in alkaline media. *J Am Chem Soc* 2014; 136: 3937–3945.
- Zalineeva A, Baranton S, Coutanceau C. How do Bi-modified palladium nanoparticles work towards glycerol electrooxidation? An in situ FTIR study. *Electrochim Acta* 2015a; 176: 705–717.
- Zalineeva A, Serov A, Padilla M, Martinez U, Artyushkova K, Baranton S, Coutanceau C, Atanassov PB. Glycerol electrooxidation on self-supported Pd<sub>1</sub>Sn<sub>x</sub> nanoparticles. *Appl Catal B* 2015b; 176: 429–435.
- Zanata CR, Fernández PS, Troiani HE, Soldati AL, Landers R, Camara GA, Carvalho AE, Martins CA. Rh-decorated PtIrO<sub>x</sub> nanoparticles for glycerol electrooxidation: searching for a stable and active catalyst. *Appl Catal B* 2016; 181: 445–455.
- Zhan Y, Xie F, Zhang H, Lin Z, Huang J, Zhang W, Sun X, Zhang Y, Chen J, Meng H. Non noble metal catalyst for oxygen reduction reaction and its characterization by simulated fuel cell test. *J Electrochem Soc* 2018; 165: J3008–J3015.
- Zhang M, Dai L. Carbon nanomaterials as metal-free catalysts in next generation fuel cells. *Nano Energy* 2012; 1: 514–517.
- Zhang X, Shen PK. Glycerol electrooxidation on highly active Pd supported carbide/C aerogel composites catalysts. *Int J Hydrogen Energy* 2013; 38: 2257–2262.
- Zhang L, Shen Y. One-pot synthesis of platinum-ceria/graphene nanosheet as advanced electrocatalysts for alcohol oxidation. *ChemElectroChem* 2015; 2: 887–895.
- Zhang L, Wang Z, Xia D. Bimetallic PtPb for formic acid electro-oxidation. *J Alloys Compd* 2006; 426: 268–271.
- Zhang J-H, Liang Y-J, Li N, Li Z-Y, Xu C-W, Jiang SP. A remarkable activity of glycerol electrooxidation on gold in alkaline medium. *Electrochim Acta* 2012a; 59: 156–159.
- Zhang Z, Xin L, Li W. Electrocatalytic oxidation of glycerol on Pt/C in anion-exchange membrane fuel cell: cogeneration of electricity and valuable chemicals. *Appl Catal B* 2012b; 119: 40–48.
- Zhang Z, Xin L, Li W. Supported gold nanoparticles as anode catalyst for anion-exchange membrane-direct glycerol fuel cell (AEM-DGFC). *Int J Hydrogen Energy* 2012c; 37: 9393–9401.
- Zhang Z, Xin L, Li W, Ja CBE. Electrocatalytic oxidation of glycerol on Pt/C in anion-exchange membrane fuel cell: cogeneration of electricity and valuable chemicals. *Appl Catal B* 2012d; 119: 40–48.

Zhang Z, Xin L, Qi J, Wang Z, Li W. Selective electro-conversion of glycerol to glycolate on carbon nanotube supported gold catalyst. *Green Chem* 2012e; 14: 2150–2152.

Zhang C, Mahmood N, Yin H, Liu F, Hou Y. Synthesis of phosphorus-doped graphene and its multifunctional applications for oxygen reduction reaction and lithium ion batteries. *Adv Mater* 2013a; 25: 4932–4937.

Zhang J, Shangguan L, Shuang S, Dong C. Electrocatalytic oxidation of formaldehyde and methanol on Ni(OH)<sub>2</sub>/Ni electrode. *Russ J Electrochem* 2013b; 49: 888–894.

Zhang W, Chuu C-P, Huang J-K, Chen C-H, Tsai M-L, Chang Y-H, Liang CT, Chen YZ, Chueh YL, He JH, Chou MY, Li LJ. Ultrahigh-gain photodetectors based on atomically thin graphene-MoS<sub>2</sub> heterostructures. *Sci Rep* 2014; 4: 3826.

Zhang J-H, Zhu T, Liang Y-J, Zhang C-J, Shi S-T, Xu C-W. CeO<sub>2</sub> promoted Au/C catalyst for glycerol electro-oxidation in alkaline medium. *J Energy Inst* 2016a; 89: 325–329.

Zhang X, Chen Y, Wang J, Zhong Q. Nitrogen and fluorine dual-doped carbon black as an efficient cathode catalyst for oxygen reduction reaction in neutral medium. *ChemSelect* 2016b; 1: 696–702.

Zhang H-J, Zhang X, Yao S, Hu H, Ma Z-F, Yang J. Simultaneous doping of nitrogen and fluorine into carbon (NFC) as metal-free oxygen reduction electrocatalysts. *J Electrochem Soc* 2017a; 164: H1081–H1085.

Zhang M, Shi J, Ning W, Hou Z. Reduced graphene oxide decorated with PtCo bimetallic nanoparticles: facile fabrication and application for base-free oxidation of glycerol. *Catal Today* 2017b; 298: 234–240.

Zhao Y, Nakamura R, Kamiya K, Nakanishi S, Hashimoto K. Nitrogen-doped carbon nanomaterials as non-metal electrocatalysts for water oxidation. *Nat Commun* 2013; 4: 2390.

Zhiani M, Rostami H, Majidi S, Karami K. Bis (dibenzylidene acetone) palladium (0) catalyst for glycerol oxidation in half cell and in alkaline direct glycerol fuel cell. *Int J Hydrogen Energy* 2013; 38: 5435–5441.

Zhou Y, Shen Y. Selective electro-oxidation of glycerol over Pd and Pt@ Pd nanocubes. *Electrochem Commun* 2018; 90: 106–110.

Zhou Y, Shen Y, Piao J. Sustainable conversion of glycerol into value-added chemicals by selective electro-oxidation on Pt-based catalysts. *ChemElectroChem* 2018; 5: 1636–1643.

Zhou Y, Shen Y, Xi J. Seed-mediated synthesis of Pt<sub>x</sub>Au<sub>y</sub>@ Ag electrocatalysts for the selective oxidation of glycerol. *Appl Catal B* 2019; 245: 604–612.

## Bionotes



**Peter Adeniyi Alaba**  
 Department of Chemical Engineering,  
 University of Malaya, 50603 Kuala Lumpur,  
 Malaysia  
[adeniyipee@live.com](mailto:adeniyipee@live.com)  
<https://orcid.org/0000-0003-3552-6718>

Peter Adeniyi Alaba obtained the Master's degree from the University of Malaya (UM), Malaysia, in 2016. He is currently a PhD candidate in the Department of Chemical Engineering, UM. His research

focuses on the transformation of sustainable feedstock such as biomass, glycerol, and CO<sub>2</sub> into energy and valuable chemicals. Specifically, he studies the kinetics, mechanisms, and structural catalytic properties for these processes. Mr. Alaba is an author and has worked in collaboration with several scientists; he has been a reviewer for several journals.



**Ching Shya Lee**  
 Department of Chemical Engineering,  
 University of Malaya, 50603 Kuala Lumpur,  
 Malaysia; and UMR5503 Laboratoire de  
 Génie Chimique (LGC), Toulouse, France  
[leecs@um.edu.my](mailto:leecs@um.edu.my)

Lee Ching Shya obtained the first degree in applied chemistry from the University of Malaya in 2003, the Master's degree from the University of Putra Malaysia in 2008, and the PhD degree in chemical engineering, majoring in electrochemistry. She holds two PhD degrees, one from the University of Toulouse and the other from the University of Malaya. She is currently a business development and commercialization officer. Her main research interests include organic synthesis, electrochemistry, reaction engineering, separation processes, and wastewater treatment.



**Wan Mohd Ashri Wan Daud**  
 Department of Chemical Engineering,  
 University of Malaya, 50603 Kuala Lumpur,  
 Malaysia  
[ashri@um.edu.my](mailto:ashri@um.edu.my)

Wan Mohd Ashri Wan Daud received the Bachelor's degree in chemical engineering from Leeds University, UK, in 1991, and the Master's degree in engineering in the field of combustion science and pollution control and the PhD degree in reaction engineering, both from University of Sheffield, UK, in 1993 and 1996, respectively. He is currently a Professor in the Department of Chemical Engineering, Faculty of Engineering, University of Malaya. His research interests include activated carbon, hydrogen production, biodiesel production, hydrodeoxygenation of pyrolytic oil, and electrocatalysis. He was the Dean for Advanced Science and Technology Cluster during 2013–2014.

## Graphical abstract

Peter Adeniyi Alaba, Ching Shya Lee,  
Faisal Abnisa, Mohamed Kheireddine  
Aroua, Patrick Cognet, Yolande Pérès and  
Wan Mohd Ashri Wan Daud

**A review of recent progress on electrocatalysts toward efficient glycerol electrooxidation**

<https://doi.org/10.1515/revce-2019-0013>

**Review:** Glycerol is a vital precursor to several value-added chemicals that are used in a wide range of applications.

**Keywords:** acidic media; alkaline media; electrocatalyst; glycerol electrooxidation; platinum.

